Chemosphere 290 (2022) 133395

Contents lists available at ScienceDirect

Chemosphere

journal homepage: www.elsevier.com/locate/chemosphere

Catalytic non-thermal plasma treatment of endocrine disrupting compounds, pharmaceuticals, and personal care products in aqueous solution: A review

Seong-Nam Nam [a,b], Choe Earn Choong [c], Shamia Hoque [a], Tanvir I. Farouk [d], Jinwoo Cho [e], Min Jang [c], Shane A. Snyder [f], Michael E. Meadows [a], Yeomin Yoon [a,*]

[a] Department of Civil and Environmental Engineering, University of South Carolina, Columbia, 300 Main Street, SC, 29208, USA
[b] Department of Civil and Environmental Engineering, Korea Army Academy at Yeong-Cheon, 495 Hoguk-ro, Kokyungmeon, Yeong-Cheon, Gyeongbuk, 38900, Republic of Korea
[c] Department of Environmental Engineering, Kwangwoon University, 447-1 Wolgye-Dong, Nowon-Gu, Seoul, Republic of Korea
[d] Department of Mechanical Engineering, University of South Carolina, Columbia, 300 Main Street, SC, 29208, USA
[e] Department of Environmental and Energy, Sejong University, Seoul, 05006, Republic of Korea
[f] School of Civil & Environmental Engineering, Nanyang Technological University, 1 Cleantech Loop, 637141, Singapore

HIGHLIGHTS

- Catalytic non-thermal plasma treatment of contaminants of emerging concern was reviewed.
- Catalytic non-thermal plasma treatment performance was significantly influenced by water quality and NTP conditions.
- Areas of future research in catalytic non-thermal plasma treatment were suggested.

GRAPHICAL ABSTRACT

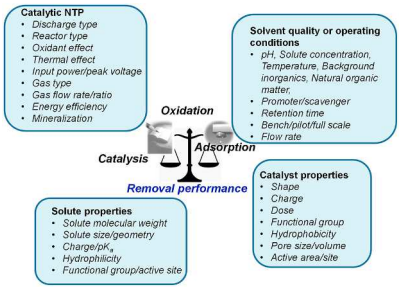

ARTICLE INFO

Handling Editor: A. Gies

Keywords:
Non-thermal plasma
Catalyst
Endocrine-disrupting compounds
Pharmaceuticals and personal care products
Water treatment

ABSTRACT

Contaminants of emerging concerns such as endocrine-disrupting compounds (EDCs) and pharmaceuticals/personal-care products (PPCPs) constitute a problem since they are not completely eliminated by traditional water and wastewater treatment methods. Non-thermal plasma (NTP) is considered as one of the most favorable treatment methods for the removal of organic contaminants in water and wastewater. The degradation of selected EDCs and PPCPs of various classes was reviewed, based on the recent literature, to (i) address the effect of the main NTP treatment parameters (water quality and NTP conditions: pH, initial concentration, temperature, background common ion, NOM, scavenger, gas type/flow rate, discharge/reactor type, input power, and energy efficiency/yield) on the degradation of contaminants and their intermediates, (ii) assess the influences of different catalysts and hybrid systems on degradation, (iii) describe EDC and PPCP degradation along with their properties, and (iv) evaluate mineralization, pathway, and degradation mechanism of selected EDCs and PPCPs for different cases studied. Furthermore, areas of potential research in NTP treatment for the degradation of EDCs and PPCPs in aqueous solutions are recommended. It could be reasonably predicted that this review is valid for

* Corresponding author.
E-mail address: yoony@cec.sc.edu (Y. Yoon).

https://doi.org/10.1016/j.chemosphere.2021.133395
Received 1 November 2021; Received in revised form 2 December 2021; Accepted 20 December 2021
Available online 21 December 2021

developing our understanding of the fundamental scientific principles concerning the catalytic NTP of EDCs and PPCPs, providing helpful and practical references for researchers and designers on the effective removal of EDCs/PPCPs and the optimized operation of catalytic NTP systems.

1. Introduction

Numerous studies have reported the occurrence of contaminants of emerging concerns (CECs), including endocrine-disrupting chemicals (EDCs) and pharmaceutical compounds (PhACs)/personal-care products (PCPs) [PPCPs], in various wastewater (WW) influents/effluents, surface waters, and finished drinking waters, where some CECs might have ecological influences even at extremely low concentrations (less than 1 μg L^{-1}) (Snyder et al., 2003; Yoon et al., 2010; Ryu et al., 2014). Since the first alarms concerning possible adverse effects of PhACs found in municipal WW treatment plants were issued by Stumm-Zollinger and Fair in 1965 (Stumm-Zollinger and Fair, 1965), several studies have

Table 1
Removal efficiencies of selected CECs at wastewater treatment plant under dry weather conditions with examples of previously published literature related to biodegradability, tendency of adsorption to sludge, and tendency of oxidation by chlorination (Ryu et al., 2014; Joseph et al., 2019).

Compound	Use	MW (g/mol)	pK_a[b]	Log K_{OW}[c]	Inf. (ng/L)	Eff. (ng/L)	Rem. (%)	Bio.	Ads.	Oxi.	Ref.
Acesulfame	Sugar substitute	201.2	2.0	−1.33	3863	3705	4	L	L	L	(Buerge et al., 2009) [B,A]; (Mawhinney et al., 2011)[O]
Atrazine	Herbicide	215.1	<2 (1.6)	2.61	ND	ND	NA	L	M	L	(Snyder et al., 2004)[B,A]; (Lei and Snyder, 2007)[O]
Atenolol	Oral beta blocker	266.3	9.6	−0.03	1040	529	49	M	L	L	(Bueno et al., 2012) [B,A]; (Huerta-Fontela et al., 2011)[O]
Benzophenone	Ultraviolet blocker	182.2	<2	3.18	88	47	47	L	M	L	(Kasprzyk-Hordern et al., 2009)[B]; (Zhang et al., 2011)[A]; (Stackelberg et al., 2007)[O]
Benzotriazole	Heterocyclic	119.2	8.2	1.44	88	47	47	M	L	L	(Reemtsma et al., 2010)[B,A]; (Sichel et al., 2011)[O]
Caffeine	Stimulant	194.2	6.1	−0.07	8810	236	97	H	H	M	(Snyder et al., 2004)[B]; (Blair et al., 2013)[A]; (Westerhoff et al., 2005)[O]
Carbamazepine	Analgesic	236.3	<2	2.45	188	156	17	L	L	H	(Clara et al., 2004)[B]; (Carballa et al., 2008)[A]; (Westerhoff et al., 2005)[O]
DEET	Insect repellent	191.3	<2	2.18	47	46	2	M	L	L	(Snyder et al., 2004)[B,A]; (Westerhoff et al., 2005)[O]
Diltiazem	Calcium channel blockers	414.5	12.9	2.79	ND	ND	NA	M	M	L	(Domenech et al., 2011)[B]; (Blair et al., 2013)[A]; (Huerta-Fontela et al., 2011)[O]
Diclofenac	Arthritis	318.1	(4.2)	0.7	6897	359	95	L	L	H	(Buser et al., 1998)[B]; (Carballa et al., 2008)[A]; (Westerhoff et al., 2005)[O]
Diphenhydramine	Antihistamine	255.5	9.0	3.27	171	142	17	L	M	NF	(Wu et al., 2010)[B]; (Hyland et al., 2012)[A]
E1	Steroid	270.4	10.3	3.13	ND	ND	NA	H	M	H	(Snyder et al., 2004)[B,A]; (Westerhoff et al., 2005)[O]
Gemfibrozil	Anticholesterol	250.2	4.7	4.72	45	33	27	H	M	H	(Snyder et al., 2004)[B,A]; (Westerhoff et al., 2005)[O]
Ibuprofen	Analgesic	206.1	4.5 (4.9)	3.97	2724	241	91	H	M	M	(Buser et al., 1999)[B]; (Carballa et al., 2008)[A]; (Lei and Snyder, 2007)[O]
Iohexol	Contrast agent	821.1	11.7	−3.05	14432	16008	−11	L	L	L	(Deblonde et al., 2011)[B,A]
Iopamidol	Contrast agent	777.1	10.7	−2.42	8518	10091	−18	L	L	NF	(Deblonde et al., 2011)[B,A]
Iopromide	Contrast agent	790.9	<2 and >13	−2.10	11133	12895	−16	L	L	L	(Snyder et al., 2004)[B,A]; (Lei and Snyder, 2007)[O]
Meprobamate	Anti-anxiety	218.3	<2	0.70	ND	ND	NA	M	L	L	(Snyder et al., 2004)[B,A]; (Lei and Snyder, 2007)[O]
Naproxen	Analgesic	230.1	4.5 (4.2)	3.18	5113	482	91	M	M	H	(Snyder et al., 2004)[B]; (Hyland et al., 2012)[A]; (Lei and Snyder, 2007)[O]
Primidone	Anticonvulsant	218.3	11.5	0.73	100	40	60	M	L	H	(Kim et al., 2012)[B]; (Ternes et al., 2002)[A]; (Huerta-Fontela et al., 2011)[O]
Propylparaben	Preservative	180.2	8.5	3.04	520	7	99	H	H	H	(Kasprzyk-Hordern et al., 2009) [B,A]; (Andersen et al., 2007)[O]
Simazine	Herbicide	201.7	1.62	2.18	ND	ND	NA	H	M	M	(Bueno et al., 2012)[B,A]; (Ormad et al., 2008)[O]
Sucralose	Sweetener	397.6	NA	−1.00	5289	4043	24	L	L	L	(Torres et al., 2011)[B,A,O]
Sulfamethoxazole	Antibiotic	253.1	2.1 & <2 (5.7)	0.89	400	117	71	L	H	H	(Snyder et al., 2004)[B,A]; (Westerhoff et al., 2005)[O]
TCEP	Fire retardant	285.5	NA	1.44	439	348	21	L	M	L	(Meyer and Bester, 2004)[B,A]; (Snyder et al., 2004)[A]; (Lei and Snyder, 2007)[O]
Triclocarban	Antibiotic	315.6	NA	4.90	198	33	83	L	H	NF	(Heidler et al., 2006)[B]; (Hyland et al., 2012)[A]
Triclosan	Antibiotic	289.6	8 (7.9)	4.76	190	63	67	L	H	H	(Snyder et al., 2004)[B,A]; (Westerhoff et al., 2005)[O]
Trimethoprim	Antibiotic	290.1	6.3, 4.0, <2 (7.1)	0.91	150	118	21	L	L	H	(Alexy et al., 2004)[B]; (Kim et al., 2005)[A]; (Westerhoff et al., 2005)[O]

Inf. = influent; Eff. = effluent; Rem. = overall removal; Bio. = biodegradation ([B]); Ads. = adsorption to sludge ([A]); Oxi. = oxidation by chlorine and/or ozonation ([O]); Ref. = references; H = high; M = medium; L = low; ND = not determined because under detection limit (ND values = 15 ng/L for E1, 50 ng/L for diltiazem, 5 ng/L for atrazine, 1.5 ng/L for simazine, and 0.5 ng/L for meprobamate); NA = not available or not applicable; NF = not found.

Table 2
Unit processes and operations used for anticipated CEC removal modified from Snyder et al. (2003).

Group	Classification	AC	BAC	O_3/AOPs	UV	Cl_2/ClO_2	NTP	Coag./floc.	FO	RO	NF	UF	Degradation {B/P/AS}*
EDCs	Pesticides	E	E	L-E	E	P-E	E	P	F-E	E	G	P–F	E {P}
	Industrial chemicals	E	E	F-G	E	P	E	P-L	F-E	E	E	P–F	G- E {B}
	Steroids	E	E	E	E	E	E	P	F-E	E	G	P–F	L-E {B}
	Metals	G	G	P	P	P	P	F-G	F-E	E	G	P–F	P {B}, E {AS}
	Inorganics	P-L	F	P	P	P	P	P	F-E	E	G	P–F	P-L
PhACs	Antibiotics	F-G	E	L-E	F-G	P-G	G-E	P-L	F-E	E	E	P–F	E {B} G-E {P}
	Antidepressants	G-E	G-E	L-E	F-G	P–F	G-E	P-L	F-E	E	G-E	P–F	G-E
	Anti-inflammatories	E	G-E	E	E	P–F	G-E	P	F-E	E	G-E	P–F	E {B}
	Lipid regulators	E	E	E	F-G	P–F	G-E	P	F-E	E	G-E	P–F	P {B}
	X-Ray contrast media	G-E	G-E	L-E	F-G	P–F	G-E	P-L	F-E	E	G-E	P–F	E {B and P}
	Psychiatric control	G-E	G-E	L-E	F-G	P–F	G-E	P-L	F-E	E	G-E	P–F	G-E
PCPs	Synthetic scents	G-E	G-E	L-E	E	P–F	G-E	P-L	F-E	E	G-E	P–F	E {B}
	Sunscreens	G-E	G-E	L-E	F-G	P–F	G-E	P-L	F-E	E	G-E	P–F	G-E
	Antimicrobials	G-E	G-E	L-E	F-G	P–F	G-E	P-L	F-E	E	G-E	P–F	F {P}
	Surfactants/detergents	E	E	F-G	F-G	P	G-E	P-L	F-E	E	E	P–F	L-E {B}

AS = activated sludge; BAC = biological activated carbon; AOPs = advanced oxidation processes; Coag./floc. = coagulation/flocculation; NTP = nonthermal plasma; *B = biodegradation, P = photodegradation, E = excellent (>90%), G = good (70–90%), F = fair (40–70%), L = low (20–40%), P = poor (<20%).

reported that various CECs are found in both WW influents and effluents at different levels, suggesting that both conventional and advanced WW treatment technologies may not completely remove all EDCs/PPCPs in WW treatment plants (Sim et al., 2011; Gao et al., 2012; Gracia-Lor et al., 2012; Mohapatra et al., 2016). Because during water and WW treatment processes the elimination of CECs could be influenced significantly by their physicochemical properties such as size/shape, solubility, functional group, pK_a, bioavailability, hydrophilicity, and polarity, investigations over the last two decades have examined the fate and transport of CECs in water and WW treatment processes (Conn et al., 2006; Benotti et al., 2009; Liu et al., 2009; Park et al., 2010; Sui et al., 2010; Yang et al., 2012; Chen et al., 2013; Luo et al., 2014; Ryu et al., 2014; Vieno and Sillanpaa, 2014).

EDCs/PPCPs are considered as potential contaminants of drinking water, especially once WW is recycled. Under the Safe Drinking Water Act, the United States Environmental Protection Agency (US EPA) requires that the Contaminant Candidate List (CCL) be updated approximately every 5 years since CCL 1 was announced in 1998 (EPA, 2021). As part of this attempt, the Endocrine Disruptor Screening and Testing Program (EDSTP) was established in 1998 to provide guidelines for screening, testing, and assessing nearly 87,000 chemicals (U.S. Department of the Interior, 2009). The EDSTP report requests for focus on possible contaminants, and that public health issues for selected compounds be confirmed via screening and testing to discover any harmful effects and determine a dose–response relationship for CECs (USEPA, 2000). While there is currently no federal regulation for PhACs in drinking water, natural water, or WW, only a few CECs (i.e., erythromycin, estrone (E1), 17b-estradiol (E2), 17a-ethinyl estradiol (EE2), and estriol (E3)) are presently listed in the US EPA's "Drinking Water CCL 4" (USEPA, 2016).

As described earlier, the removal of EDCs/PPCPs depends on their physicochemical properties and treatment methods in water and WW treatment plants. In addition, their removal is significantly influenced by various wastewater treatment techniques, conditions, and/or mechanisms (*e.g.*, biodegradation, (activate) sludge, oxidation, dilution of WW effluent/combined sewer overflow, variations in rainfall, and/or temperature) (Benotti and Brownawell, 2007; Weyrauch et al., 2010; Phillips et al., 2012). Table 1 presents both measured and estimated degrees of removal for selected EDCs/PPCPs in WW treatment plants under dry-weather circumstances, using representative samples of the current literature concerning biodegradability, along with tendencies regarding sorption to sludge and oxidation by chlorination/ozonation.

Numerous prior researches have reported that EDCs/PPCPs are eliminated to various levels by both conventional and advanced treatment techniques such as coagulation/flocculation (Westerhoff et al., 2005; Joseph et al., 2012; Jung et al., 2015), chlorination (Westerhoff et al., 2009), activated carbon (Yoon et al., 2003; Snyder et al., 2007; Jung et al., 2013), carbon nanoparticles (*e.g.*, carbon nanotubes (Joseph et al., 2011a; Joseph et al., 2011b; Zaib et al., 2012) and graphene oxides (Nam et al., 2015)), metal–organic frameworks (Jun et al., 2019a; Jun et al., 2020b), MXenes (Jun et al., 2019b; Jun et al., 2020a), membrane (Yoon et al., 2006, 2007; Heo et al., 2013), O_3 (Westerhoff et al., 2005; Moreira et al., 2015), ultraviolet (UV) radiation (Han et al., 2012; Farzadkia et al., 2014; Duan et al., 2017), sonodegradation (Rahimi et al., 2016; Rao et al., 2016; Serna-Galvis et al., 2016), non-thermal plasma (NTP) (Ansari et al., 2020), and biodegradation (Yoon et al., 2010; Ryu et al., 2011, 2014). Unlike commonly recognized advanced oxidation methods such as O_3/H_2O_2, UV/TiO_2, UV/H_2O_2, and $UV/Fe^{3+}/H_2O_2$ processes, the NTP process has lately been employed as an advanced treatment method for the elimination of complicated organic chemicals in water and WW (Gerrity et al., 2010; Ceriani et al., 2018; Feng et al., 2018; Fan et al., 2021). Table 2 summarizes the anticipated performances of different processes used in both water and WW treatment plants based on literature reports that demonstrate specific classes of compounds or compare these compounds to other EDCs/PPCPs that have been examined in detail. In plasma liquid interactions, chemical reactions occur in the bulk gas/liquid phases and at the interface, with simultaneous transport processes taking place. Plasma kinetic processes involve water form highly reactive oxidative (*e.g.,* $OH^{\bullet}$, O, $HO_2^{\bullet}$, H_2O_2, O^{2-}, etc.) and reductive species (*e.g.,* free electrons, aqueous electrons e_{aq}, H, etc.). Reductive species (*e.g.,* solvated electrons) have been reported to play an important role in the degradation of organic compounds (Mededovic Thagard et al., 2016). The demerits or problems of NTP treatment include high-level energy consumption, low efficiency, low operating pressure, and the possible production of undesirable byproducts (Kim et al., 2015a). However, the combination of plasma with various catalysts, such as TiO_2 (Zhang et al., 2017a), $ZnO/\alpha\text{-}Fe_2O_3$ (Ansari et al., 2020), Ag_3PO_4 (Gong et al., 2020), and ZrO_2/CeO_2 (Reddy and Subrahmanyam, 2015), could overcome the drawbacks. The majority of studies undertaken after year 2000 have focused on catalytic NTP processes to find answers to these problems. The effect of NTP combined with catalysts improves the production of various types of oxidative/reductive species based on two potential behaviors: (i) catalysts are introduced to the discharge zone, inducing heterogeneous reactions in the system owing to the interaction of catalyst and plasma and (ii) catalysts are introduced upstream or downstream of the discharge region (Russo et al., 2020).

Over the last two decades, studies have evaluated the elimination of EDCs/PPCPs by various NTP treatments. The few current reviews on catalytic NTP treatment (Kim et al., 2015a; Feng et al., 2018; Russo

et al., 2020) focuses on the removal of volatile organic compounds and NO_x, and reports only a few compounds in water. Therefore, a complete review of EDC/PPCP removal by catalytic NTP treatment is important because degradation of EDCs/PPCPs is affected by unique properties of solute and catalyst, as well as by solvent quality and NTP operating conditions. The main purpose of this review is to explore recent efforts of NTP processes combined with various catalysts in water/WW treatment and reveal the differences and restrictions, in order to underline forthcoming study areas based on the latest and appropriate studies. Particularly, this review aims to (i) identify the main parameters (water quality conditions—pH, initial concentration, temperature, background common inorganics, natural organic matter (NOM), and promoters/scavengers—and NTP operating conditions—discharge type, reactor type, input power, peak voltage, gas type, retention time, and gas flow rate/ratio) that affect the degradation and byproducts of EDCs/PPCPs during catalytic NTP treatment, (ii) assess the effects of various catalyst properties (charge, dose, functional group, hydrophobicity, pore size/volume, and active area/site) and hybrid processes on degradation, and (iii) evaluate EDC and PPCP removal according to their types/properties (molecular weight, charge/pK_a, hydrophilicity, and functional group) during catalytic NTP treatment.

2. Catalytic NTP treatment of various EDCs/PPCPs

2.1. Removal influenced by water quality and NTP conditions

2.1.1. pH, initial concentration, and temperature

pH: In general, surface water, groundwater, and municipal/industrial wastewater have different pH values. The solution pH significantly influences both the physicochemical properties of compounds and the formation of active species in dielectric barrier discharge (DBD) treatment (Liu et al., 2018). The removal rates of fluocinolone acetonide, triamcinolone acetonide, and clobetasol propionate varied from approximately 60 to 75%, 50–70%, and 60–75%, respectively, for an initial pH of 3.3–8 (Liu et al., 2019). The degradation degrees of three contaminants were in the following order at various pH conditions at a reaction of 2 h: 6.8 > 4.6 > 8.0 > 3.3. The rate constants of fluocinolone acetonide, triamcinolone acetonide, and clobetasol propionate increased from 0.001 to 0.013, 0.004 to 0.010, and 0.010 to 0.012 min^{-1}, respectively, with an increase in initial pH from 3.3 to 4.6. These results suggest that the relatively weak acidic condition of pH 4.6–6.8 is conducive for degradation by DBD treatment. The highest degradation of 2,4-dichlorophenol was observed at pH 6 in varying pH conditions (3–8) (Zhang et al., 2018a), a finding that is comparable with the above. At very low pH conditions, the formation of H_2O_2 appeared to be dominant compared to that of $OH^•$ (Gai, 2007). The oxidation degree of H_2O_2 was approximately 100 times less than that of $OH^•$ (Gai, 2007), which resulted in a reduction in the degradation rate. With an increase in pH to over 4.6, the concentration of hydroxide ions increased. Therefore, hydroxide ions might act as scavengers of $OH^•$, which leads to reduction of the contaminant degradation efficiency (Jiang et al., 2012). In contrast, self-decay of H_2O_2 might improve at relatively high pH environments, resulting in reduction of the oxidation capability (Singh et al., 2016). In addition, due to the high pK_a values of fluocinolone acetonide, triamcinolone acetonide, and clobetasol propionate (13.9, 11.8, and 13.6, respectively), their molecules have a tendency to reduce their molecular states and appear more challenging to be attacked by $OH^•$ in alkaline conditions (Liu et al., 2019).

Initial concentration: It is widely known that the solute initial concentration affects the transport and fate of contaminants during DBD processes (Russo et al., 2020). The initial concentration of the solution showed a substantial influence on phenol degradation during DBD treatment (Wu et al., 2020). As the phenol concentration increased to 20, 30, 40, 50, and 60 mg L^{-1} over a reaction time of 20 min, the degradation efficiency slowly decreased to 57, 33, 24, 20, and 18%, respectively. These findings are somewhat comparable with that of a previous study (Ceriani et al., 2018).

To assess whether the DBD process showed a synergistic or unfavorable performance for the mixed contaminant removal process, various tests were performed by varying the initial concentrations of three different contaminants (diclofenac, carbamazepine, and ciprofloxacin) from 1000 to 10,000 μg L^{-1}, which are relatively higher contaminant concentrations compared to those typically found in surface waters (Singh et al., 2017a). From the initial tests, insignificant variation was observed between the contaminants in single and mixed conditions at relatively lower concentrations. Arriving at a clear conclusion from the behavior of contaminant removal, particularly in mixed conditions, seemed unlikely. To achieve a concentration of 1000 μg L^{-1} of mixed PhACs, 333 μg L^{-1} each of diclofenac, carbamazepine, and ciprofloxacin were required. Comparably, to achieve concentrations of 4000 and 10,000 μg L^{-1} of mixed PhACs, the individual PhACs (diclofenac, carbamazepine, and ciprofloxacin) were mixed in the same ratio. The treatment time necessary for the total removal of the mixture of contaminants, each of concentration 333 μg L^{-1}, was equal to the treatment time necessary for the removal of 1000 μg L^{-1} each of diclofenac, carbamazepine, and ciprofloxacin as individual PhACs. Nevertheless, at the higher original concentrations of the mixed system, removal time was greater compared to the treatment time necessary for individual contaminant systems. The reaction rates (k) of diclofenac, carbamazepine, and ciprofloxacin in single PhAC removal systems were greater than their reaction rates in the mixed PhAC system. The findings suggest that these PhACs demonstrated unfavorable influence in mixed conditions for the original concentrations of 4000 and 10,000 μg L^{-1} (Singh et al., 2017a).

Temperature: Solution temperature plays an important role in activated persulfate treatment (Ji et al., 2015). During heat-activated persulfate treatment, the degradation rate of atrazine was approximately 15%, 20%, 25%, and 75% at 20 °C, 25 °C, 35 °C, and 45 °C, respectively (Wang et al., 2021). Increasing the temperature from 20 to 25 °C resulted in an improvement of the rate constant from 0.002 to 0.019 min^{-1}. The removal rate of atrazine increased remarkably as the solution temperature increased from 15 to 25 °C during heat-activated the DBD/microbubble/persulfate treatment (Tan et al., 2012). The removal efficiency was 89% (0.027 min^{-1}) once the temperature of the DBD/microbubble/persulfate process reached 25 °C in 75 min. However, atrazine degradation with only heat activation at the same temperature was much lower (26% and 0.004 min^{-1}). This could be due to the cleavage of the peroxide bond (140 kJ mol^{-1}) to produce $SO_4^{-•}$ as a result of the relatively high temperature (>45 °C) (Wang and Wang, 2018). In accordance with the conditions for endothermic reaction, the heat absorbed by the solution was 6.3 kJ, which increased the solution temperature from 20 to 35 °C, accounting for nearly 17% of the total power and 25% of atrazine degradation. Thus, the heat produced by the DBD treatment was beneficial for atrazine degradation (Wang et al., 2021).

2.1.2. Background common ion, scavenger, and NOM

Background common ion: Various cations and anions exist in both natural waters and industrial wastewater, including Cl^-, Na^+, Ca^{2+}, SO_4^{2-}, HCO_3^-, Fe^{2+}, and Mn^{2+}. The removal rate of atrazine with DBD treatment increased apparently with the addition of Fe^{2+} (Feng et al., 2016). The first-order rate constant of atrazine degradation in the presence of 0.6 mmol L^{-1} of Fe^{2+} was 0.47 min^{-1}, which was approximately three times greater than that in the absence of Fe^{2+} (0.17 min^{-1}). The increased removal rate of atrazine in the presence of Fe^{2+} might be described by the traditional Fenton reaction that generates the radicals $HO^•$ and $HO_2^•$. However, the degradation rate constant reduced to 0.38 min^{-1} with an increase in Fe^{2+} concentration to 1.2 mmol L^{-1}, indicating that excess addition of Fe^{2+} had a negative impact on the removal of atrazine. The reduced removal efficiency of atrazine with extra addition of Fe^{2+} was possibly due to the competition between Fe^{2+} and atrazine for $HO^•$ (Brillas et al., 2009). The presence of NO_3^-, PO_4^{3-}, and

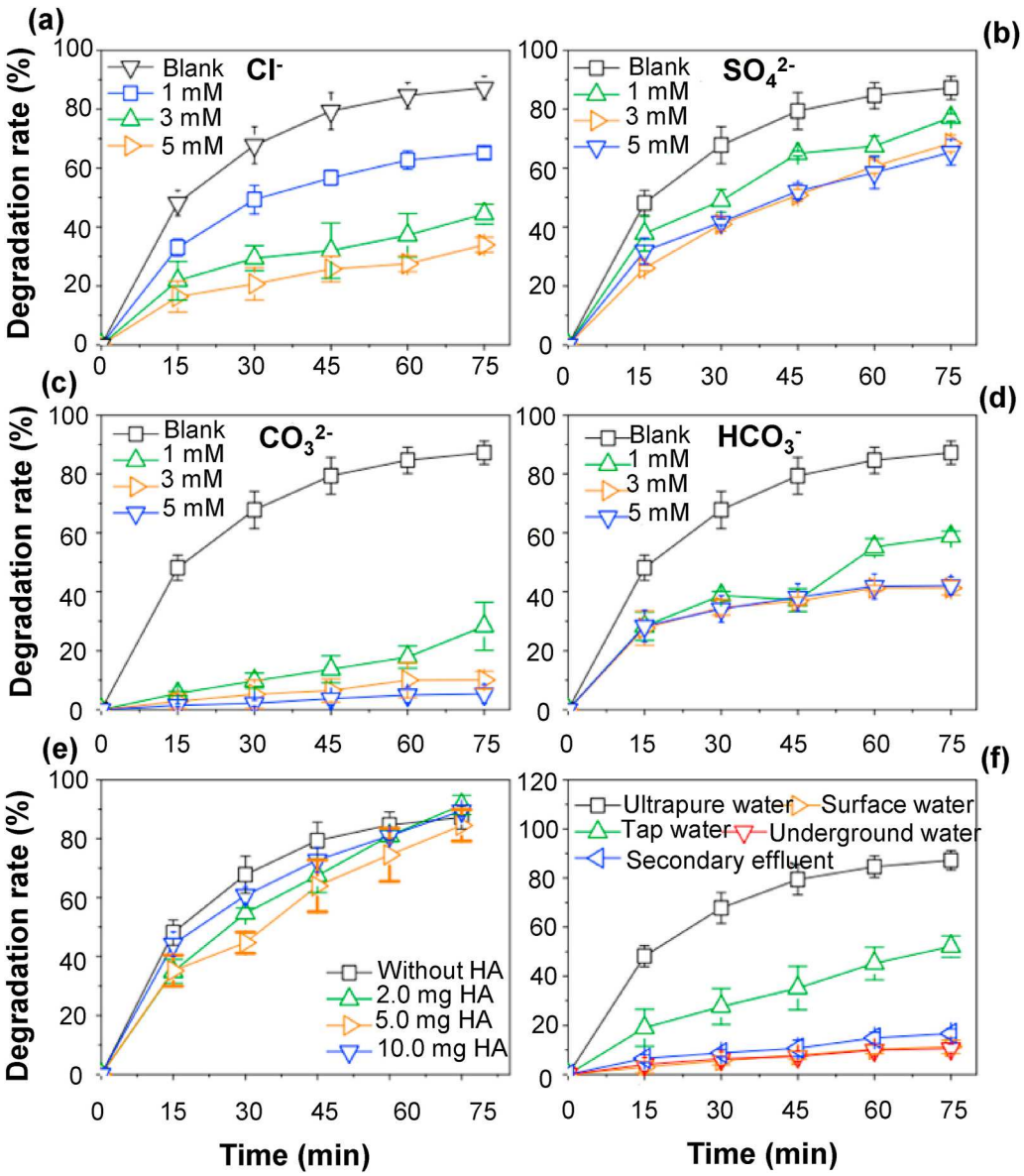

Fig. 1. Effect of ions and mechanism diagrams of ion additions during DBD/microbubbles (MBs)/persulfate (PS) treatment for atrazine (ATZ) removal: (a) Cl^-, (b) SO_4^{2-}, (c) CO_3^{2-}, (d) HCO_3-, (e) humic acid (HA), (f) the real water matrix (unadjusted pH); (power = 85 W, pH = 7.0 ± 0.2, air flow = 30 mL/min, [PS] = 1 mM, [ATZ] = 5 mg) (Wang et al., 2021).

SO_4^{2-} showed somewhat of an insignificant influence on the total degradation efficiency of 2,4-dichlorophenoxyacetic acid removal during DBD treatment (Singh et al., 2017b).

During a DBD/microbubble/persulfate hybrid process, atrazine degradation rates decreased in surface water, underground water, and secondary WW effluents, while much higher degradation rates were observed with tap water (52%) and deionized ultrapure water (87%), as shown in Fig. 1 (Wang et al., 2021). The results clearly indicate the potential inhibition mechanisms of natural water. The influences of different inorganic and organic compounds, such as SO_4^{2-}, Cl^-, HCO_3^-, and CO_3^{2-}, and humic acid on atrazine degradation were additionally explored at varying ion concentrations (1–5 mM). The degradation rate of atrazine was reduced by 34% with increasing chloride ions, which was presumably due to the additional reactions between Cl^- and $SO_4^{-\bullet}/OH^\bullet$, leading to the generation of reactive species, including HOCl, OCl^-, $Cl^\bullet$, and $Cl_2^{-\bullet}$ (Fan et al., 2015). While chlorine-free radicals could react with electron-rich molecules, these reactive species have restricted oxidizing capacities for atrazine degradation (Liu et al., 2013). Atrazine degradation decreased by 22% in the presence of sulfate ions, because SO_4^{2-} consumed $OH^\bullet$ and H^+ to generate $SO_4^{-\bullet}$ and other free radicals (Zhang et al., 2017b). The unfavorable influence of alkalinity on atrazine degradation could be attributed to the formation of $CO_3^{-\bullet}$ by the additional reactions between HCO_3^-/CO_3^{2-} and $OH\cdot/SO_4^{-\bullet}$ (Liang et al., 2006). In addition, the degrees of CO_3^{2-} entrapping of $OH\cdot/SO_4^{-\bullet}$ were quicker than those of HCO_3^- (Liu et al., 2013), which might explain its greater unfavorable influence compared to HCO_3^-.

Scavenger and NOM: In a study to verify the essential role of oxygen radicals such as $OH^\bullet$ in the removal process of bisphenol A, the degradation efficiency decreased in the presence of a radical scavenger (*tert*-butanol) (Sarangapani et al., 2017a). The findings showed that the degradation rate decreased by approximately 20% with the addition of the scavenger. In addition, the presence of the radical scavenger caused a reduction in the rate constant from 0.189 min^{-1} to 0.098 min^{-1} at a peak voltage of 80 kV. The findings suggest that there was a competition for $OH^\bullet$ between tertiary butanol and bisphenol A, which inhibited the interaction between $OH^\bullet$ and the bisphenol A molecule (Sarangapani et al., 2017a). The presence of various radical scavengers such as *tert*-butanol, isopropyl alcohol, and Na_2CO_3 significantly reduced the

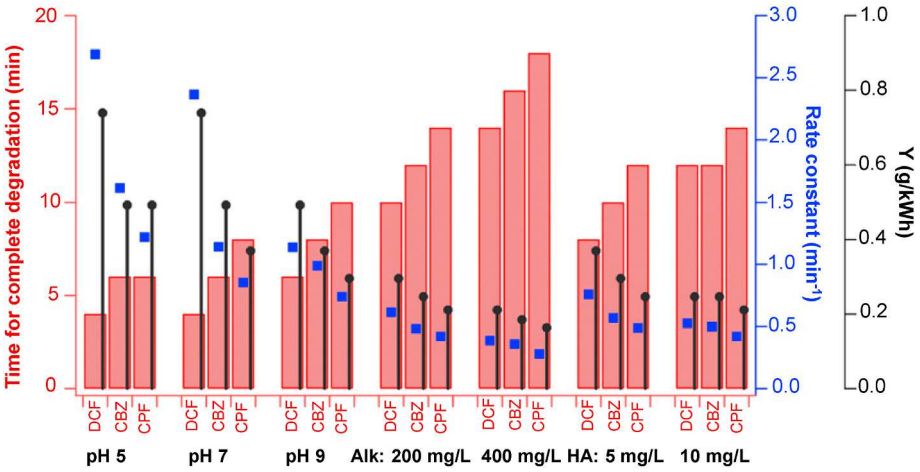

Fig. 2. Effect of pH and radical scavengers on PhACs degradation time, rate of reaction and degradation yield; Initial concentration of PhACs ¼ 1 mg/L; Power delivery ¼ 101.5 W (Corresponding voltage and frequency were 25 kV and 25 Hz). All the experiments were performed in triplicates and average values were used to plot the graph. DCF = diclofenac, CBZ = carbamazepine, and ciprofloxacin (Singh et al., 2017a).

degradation efficiency of atrazine (Feng et al., 2016). The removal efficiency of atrazine in the presence of *tert*-butyl alcohol, isopropyl alcohol, and Na_2CO_3 decreased by approximately 50, 40, and 30%, with a rate constant of 0.08, 0.07, and 0.05 min^{-1}, respectively.

The oxidation degradation of contaminants is frequently impacted by commonly found radical scavengers such as alkalinity and humic acid (Jiang et al., 2014). In the presence of an alkalinity of 400 mg L^{-1} or humic acid of 10 mg L^{-1}, the entire removal of three different PhACs (diclofenac, carbamazepine, and ciprofloxacin) occurred in 14, 16 and 18 min of contact time, respectively (Fig. 2) (Singh et al., 2017a). Owing to the competition that occurs between PhACs, intermediates, and background inorganics/organics, the rate of reactive species produced is always insufficient to oxidize all the organic contaminants. Thus, the degree of PhAC removal decreases with increasing concentration of these scavengers. A previous study reported that the degree of generation of the oxidants $OH^{\bullet}$ and H_2O_2 is mainly influenced by radical scavengers (Singh et al., 2016). Consequently, with increase in alkalinity and NOM, the degree of generation of $OH^{\bullet}$ and H_2O_2 decreases, resulting in reduction in the removal rate. It could be presumed that the property of radical scavenging substantially affect the removal rates of contaminants (Singh et al., 2017a). Humic acid is one of the prevalent components of NOM in an aquatic environment. Significantly low degradation of atrazine was observed in the presence of 5-mg L^{-1} humic acid (Wang et al., 2021), which could be attributed to the scavenging effect of humic acid on $OH^{\bullet}$ and $SO_4^{-\bullet}$ (Liang et al., 2006).

2.1.3. Gas type and gas flow rate

Feed gas could affect the removal of contaminants in plasma reactors, as it might influence the generation of various oxidants and positively/negatively charged ions (Reddy and Subrahmanyam, 2015). In comparison to air plasma treatment in a continuous-flow pulsed DBD reactor with a mixture of various contaminants, approximately 5–10% greater degradation rate was observed in Ar plasma, and about 15–20% greater degradation was achieved when the discharge was controlled in O_2 (Wardenier et al., 2019). Clearly, shifting the feed gas from air to O_2 provided a valuable way to improve the effectiveness of contaminant degradation in the reactor. The significant change in effectiveness achieved between air and O_2 plasmas suggests that different chemical species could be produced in various quantities under air and O_2 atmospheres (Lukes et al., 2005). The degrees of O_3 production in various feed gases were comprehensively reported in a previous study [28]. In particular, the study reported that by changing the feed gas from O_2 to air, the total quantity of O_3 produced in the discharge decreased by nearly 25%. This substantially reduced O_3 generation was attributed to the presence of N_2 in the discharge medium, which enabled the creation of NO, whose availability in huge quantities of NO is very undesirable as it rapidly results in O_3 and subsequently NO_2 formation (Kogelschatz, 2003).

Slightly different results were observed for the removal of three different glucocorticoids (fluocinolone acetonide, triamcinolone acetonide, and clobetasol propionate) by the DBD process (Liu et al., 2019). The highest degradation was achieved with the plasma-working gas of Ar, followed by the working gas of N_2 or O_2. In various kinds of discharge working gases, the production rate of $OH^{\bullet}$ varied during the DBD process (Cui et al., 2019). The production rate of $OH^{\bullet}$ diminished in the order $Ar > N_2 > O_2$ in the DBD system, which was in agreement with the degradation efficiency of the three contaminants. A separate study showed that additional reactive oxygen species appeared to be produced at higher ratios of O_2 using DBD plasma with a combined working gas of O_2 and N_2 (Takahashi et al., 2016). Zhang et al. examined the influences of O_2 ratio on norfloxacin removal by DBD plasma and discovered that the removal rate increased with increasing O_2 amount up to 40% (Zhang et al., 2018b).

Owing to the faster contaminant degradation for plasma discharges maintained in O_2 gas compared to discharges maintained in Ar and air, the effect of three different O_2 flow rates on the degradation of eight contaminants showed that by reducing the O_2 flow rate from 1.0 to 0.1 standard L min^{-1}, the removal rate of each contaminant was reduced by approximately 5–10% (Wardenier et al., 2019). At a gas flow rate of 0.1 L min^{-1}, 95% of atrazine was removed, while no less than 97% removal was achieved for dichlorvos, bisphenol A, carbamazepine, and EE2. However, the electrical energy per order increased with an increasing gas flow rate, giving electrical energy per order values between 9.4 kWh m^{-3} (atrazine) and 6.8 kWh m^{-3} (EE2). The favorable influence of improved contaminant degradation and greater energy efficiency with smaller flow rates was clearly due to the greater retention time of the O_2 gas in the discharge zone where a higher quantity of active species was expected to be formed (Ognier et al., 2009).

2.1.4. Discharge/reactor type, input power, and energy efficiency/yield

Discharge reactor and type: In the last two decades, numerous reactor configurations employing various electrical excitation approaches and gases have been designed (Malik, 2010; Stratton et al., 2015). Three main methods, namely immediate electrical liquid discharges, electrical discharges over liquid surface, and discharges in bubbles/vapor in solutions, were examined, with hybrid configuration systems that employed bubbles or mixed gas–liquid phases revealing maximum energy efficiency (Jiang et al., 2014). A separate study examined remotely

generated plasmas, where the plasmas were produced outside of their liquid phases and their radical products were bubbled into the liquids (Vanraes et al., 2015a). While the theory is very comparable to ozonation, the essential distinction is that the bubbled gas included additional reactive species, such as H_2O_2 and $OH^{\bullet}$. It was determined that these reactors could compete with other designs such as the hybrid approaches with the plasma formed in the gas–liquid phase (Walsh and Bruggeman, 2011). However, there is no information on direct evaluation of various energization methods for remotely generated plasmas achieved in identical experimental systems. This is critical, since it is widely recognized that the effectiveness of discharge varies depending on the reaction area between plasma and liquid. Bosi et al. described this matter by evaluating, characterizing, and comparing the degradation efficiency of phenol in a plasma reactor with two different configurations—"hybrid" pin-to-plate streamer and "remote" DBD (Bosi et al., 2018). The findings suggest that the impacts of local and bulk temperature and, probably also, the catalytic influences of metal particles and/or ions generated by sputtering/erosion of the electrode tip could contribute to greater effectiveness of the streamer-based treatment compared with the DBD process.

Input power: Input power is a significant operation parameter in a DBD process because it affects the production efficiency and quantity of high-energy electrons, which directly governs the generation of reactive oxidizing substances O_3/O·/$OH^{\bullet}$, nitrogen radicals, and also contribute to UV irradiation (Wang et al., 2016b). The removal of *N*,*N*-diethyl-m-toluamide at various discharge voltages (12, 15, and 18 kV) and an initial concentration of 20,000 μg L^{-1} was compared (Yu et al., 2017). The removal of *N*,*N*-diethyl-m-toluamide clearly increased with increasing discharge voltage, reaching 65, 77, and 81% at 12, 15, and 18 kV, respectively, for a treatment time of 27 min. The rate constant also increased from 0.036 to 0.063 min^{-1} with an increase in the discharge voltage from 12 to 18 kV. The discharge voltage showed a substantial influence on the generation of reaction species, with their intensity generation degree varying depending on the discharge voltage (Kornev et al., 2006). It was reported that the removal rate of acetaminophen could be gradually improved by increasing the input voltage from 18 to 24 kV (Zhang et al., 2017a). In particular, with an initial concentration of 20 mg L^{-1}, the degradation rate of acetaminophen increased from 50 to 65% with an increase in input power from 18 to 20 kV, respectively. Once the input power was greater than 20 kV, acetaminophen degradation increased substantially, reaching 78 and 95% at 22 and 24 kV, respectively. The energy yield decreased slightly with increasing input power (from 57 mg kWh^{-1} at 18 kV to 46 mg kWh^{-1} at 24 kV). The finding was anticipated because it is difficult to achieve the highest degradation rate and greater energy yield simultaneously without an additional catalyst (Wang et al., 2016b). Additionally, the enhanced input power resulted in increased energy waste, indicating that further electrical energy was transformed into heat.

The removal efficiency of various contaminants varied between approximately 90 and 96% at a power of 40 W, and improved to 97–99% at 65 W, with the target contaminants totally degraded at 77.5 and 90 W (Wardenier et al., 2019). This can be attributed to an increase in electron production due to increase in power. In particular, the greater rate of contaminant degradation at higher power was presumably due to improved $OH^{\bullet}$ generation, a result that is somewhat consistent with that of a previous study in which $OH^{\bullet}$ production nearly increased linearly with increasing discharge power in pulsed corona plasma (Ono and Oda, 2002). Despite the enhanced contaminant degradation rate at elevated power settings, it was found that the energy efficiency somewhat increased by approximately 10–15% for atrazine, alachlor, dichlorvos, diuron, pentachlorophenol, and bisphenol A with an increase in power from 40 to 65 W, while a slight decrease was observed for carbamazepine and EE2. These findings suggest that the impact of power on energy efficiency is presumably compound-specific and appears to be restricted to certain power ranges (Wardenier et al., 2019). Liu et al. showed that the removal efficiency of three different glucocorticoids in a continuous DBD reactor with a contact time of 2 h at 58 W was approximately 80–85%, while the degradation increased with increasing discharge power (36–58 W) (Liu et al., 2019). As described earlier, in addition to the relatively high production of electrons and free radicals under high power conditions, the increased discharge power significantly enhanced the dissociation/ionization/excitation of target molecules, which resulted in production of more reactive species such as O_3 (Kim et al., 2013). In addition, as the discharge power increased, the UV intensity became higher, leading to the production of additional $OH^{\bullet}$ (Hu et al., 2019).

Energy efficiency and yield: Determining the energy efficiency of an NTP process is always significant for practical applications in water and WW treatment. The degradation efficiency can be described by the quantity of contaminants removed per unit of energy consumed. The amount of energy required depends on the nature of the discharge reactor, initial solute concentration, and properties of each compound (Reddy et al., 2014). The energy consumed during E1, E2, and bisphenol A degradation decreased from 0.777×10^{-3} to 0.737×10^{-3}, 1.01×10^{-3} to 0.810×10^{-3}, mg kWh^{-1} for bisphenol A, E1, and E2, respectively with an increase in applied voltage from 60 to 70 kV (Sarangapani et al., 2017a). These values are somewhat relatively low compared with the results of similar studies using DBD reactors, presumably due to its high initial solute concentration (2000 μg L^{-1}), large sample volume, and large amount of background organic matter (Gao et al., 2013). In general, advanced oxidation processes with chemical addition require high energy consumption (Jiang et al., 2012). For instance, when approximately 80% photocatalytic degradation of methyl orange was achieved with mesoporous-assembled TiO_2 for a contact time of 240 min, the energy cost and reaction time were much greater than when the same degradation was achieved with the NTP process (Jantawasu et al., 2009). Unlike the UV/H_2O_2 and O_3/H_2O_2 methods, the main advantage of DBD plasma is the ability to produce UV light and oxidizing species, such as O_3 and $OH^{\bullet}$, with no chemical addition or utilization of a UV lamp (Jiang et al., 2012).

The energy yield of contaminant degradation by an NTP process for three different glucocorticoids (approximately 4–6 mg kWh^{-1}) (Liu et al., 2019) was greater than that by photocatalysis combined with TiO_2 (1.8 mg kWh^{-1}) (Ohko et al., 2001) and catalytic plasma with a tubular reactor (0.24 mg kWh^{-1}) (Cui et al., 2019). In addition, the energy yield of various NTP processes might be enhanced by combining them with catalysts. An outstanding energy efficiency was achieved during DBD treatment for carbamazepine removal, which could be ascribed to the use of a large reactor and the extremely low concentration of carbamazepine (176 ng L^{-1}) (Singh et al., 2019). While electrical energy required for unit contaminant removal describes the energy efficiency in terms of the volume of the reactor, energy yield defines the energy efficiency in terms of contaminant degradation. The observed energy yield of carbamazepine degradation in deionized water was between 16 and 36.8 mg kWh^{-1}, which is similar to previously obtained values (3–45 mg kWh^{-1}) (Banaschik et al., 2015). In an identical DBD treatment reactor, a much greater energy yield (760 mg kWh^{-1}) was obtained at a greater diclofenac concentration of 50 mg L^{-1} (Singh et al., 2019). Comparable energy yield values (approximately 19 and 45 mg kWh^{-1}) were found in DBD-based plasma treatment processes for carbamazepine degradation at a concentration of 23.6 mg L^{-1} (Krause et al., 2011). A much greater energy yield value (180 mg kWh^{-1}) was obtained in a falling liquid film DBD treatment system (Liu et al., 2012a), which might be ascribed to the greater contact area between the plasma and liquid. These findings suggest that energy efficiency and yield are significantly affected by the reactor type, treatment settings, and contaminant type/concentration.

2.2. Removal influenced by catalysts

Some recent studies have reported that NTP treatment integrated with different catalysts improves the production of various active species and the activity and stability of the catalysts (Krause et al., 2009;

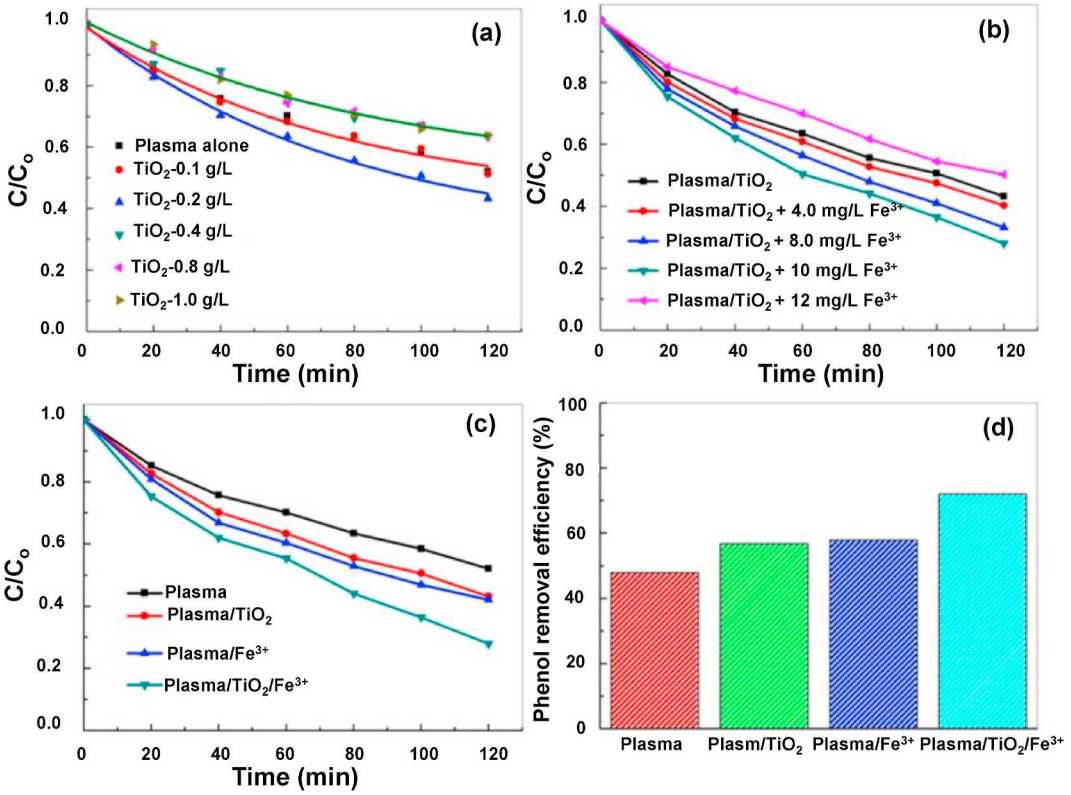

Fig. 3. (a) Effect of TiO_2 dosage on degradation of phenol by pulsed discharge; (b) Effect of Fe3+ dosage on phenol degradation in plasma/TiO_2 system; (c) The changes of phenol concentration in plasma, plasma/TiO_2, plasma/Fe^{3+}, and plasma/TiO_2/Fe^{3+}, respectively; (d) Phenol removal efficiency in plasma, plasma/TiO_2, plasma/Fe^{3+}, and plasma/TiO_2/Fe^{3+}, respectively (Duan et al., 2018).

Reddy et al., 2014; Zhang et al., 2017a; Giardina et al., 2018; Tang et al., 2018a; Wang et al., 2018, 2019; Ansari et al., 2020; Gong et al., 2020; Lou et al., 2021). The degradation of triclocarban in water by DBD plasma integrated with TiO_2-coated activated carbon fibers as catalysts was examined at atmospheric pressure (Wang et al., 2016a). TiO_2--coated activated carbon fibers employed in this study were cut in a circular form, with the fiber diameter equal to the diameter of the circular form. The influence of the size of the TiO_2-coated activated carbon fibers on the degradation of triclocarban was explored by modifying the fiber diameter, with the depth of the catalyst layer roughly 2 mm. The results demonstrated that the removal efficiency of triclocarban was substantially enhanced with an increasing diameter of TiO_2-coated activated carbon fibers. In particular, when the diameter of the composite catalysts reached 6 cm, the degradation rate constant was 0.283 mg L^{-1} min^{-1} and the treatment time was 30 min. Since the TiO_2-coated activated carbon fibers were cut in a circular form, the larger diameter of catalysts intended greater TiO_2 coated activated carbon fibers. With the increasing diameter of TiO_2-coated activated carbon fibers, TiO_2 was greatly irradiated by UV light to generate additional active radicals, which definitively caused a significant enhancement of the degradation efficiency of triclocarban in water (Wang et al., 2016a). These findings suggest that composite catalysts can provide constant charges, which might improve the degradation efficiency of triclocarban in DBD/TiO_2-coated activated carbon fiber reaction systems (Xin et al., 2016).

The influences of TiO_2 and Fe^{3+} concentrations on phenol removal were explored (Duan et al., 2018). For various TiO_2 concentrations (0.1–1.0 g L^{-1}), the highest degradation rate of phenol was achieved at a concentration of 0.2 g L^{-1} (Fig. 3). In general, this finding can be ascribed to the fact that the intensity of photo-generated e^-–h^+ pairs and $OH^•$ increases with increasing TiO_2 concentration, resulting in elevated photocatalytic effectiveness. Nevertheless, when the concentration of TiO_2 exceeds the optimum level, the properties of the TiO_2 particle affects the start and transmission of the discharge in the liquid stage (Konstantinou and Albanis, 2004). At an optimum TiO_2 dose of 0.2 g L^{-1}, phenol removal improved initially, but subsequently reduced with increasing Fe^{3+} concentration until an optimum value of 10 mg L^{-1} was reached. The initial degradation enhancement in the presence of Fe^{3+} was presumably because the Fe^{3+} ions served both as an e^-/h^+ trap and a recombination base (Hao and Zhang, 2009). A few additional experiments to determine the synergetic influence of Fe^{3+} and TiO_2 on photocatalytic degradation showed that the degradation rate of phenol was substantially enhanced in the presence of Fe^{3+} and TiO_2 in pulsed discharge treatment. The synergetic influence can be explained by two reasons: (i) Ti^{4+} can be substituted by Fe^{3+} in a TiO_2 lattice, which influences the light absorption behavior of TiO_2 and charge separation between e^- and h^+; and (ii) Fenton-like reaction can occur due to the reduction of Fe^{3+} to Fe^{2+} by a photoelectron on the TiO_2 surface, which enhances the formation rate of $OH^•$ in a plasma process integrated with TiO_2 and Fe^{3+} (Duan et al., 2018).

DBD integrated with Fe-based zeolite as a catalyst was employed at various concentrations (400–2000 mg L^{-1}) to degrade phenol in WW (Wu et al., 2020). While a high concentration caused a high degradation efficiency at the initial reaction stage, the phenol degradation efficiency slowly plateaued out in the later stage. Wang et al. reported that plasma combined with a metal catalyst could improve the degradation of ammonia, with a powerful synergy established by the plasma and the metal catalyst (Wang et al., 2015). These results can be ascribed to the ability of the metal oxide incorporated on the surface of the Fe-based zeolite to interact with H_2O to produce hydroxyl functional groups, which can generate $OH^•$ by reacting with O_3 during the DBD treatment process (Wu et al., 2020). A separate study reported that the gas phase of DBD plasma combined with TiO_2-reduced graphene oxide significantly improved acetaminophen degradation from approximately 50 to 90%

(Zhang et al., 2017a). The acetaminophen removal rate was substantially affected by several parameters such as input power, solution pH, dose, and mass ratios of TiO_2-reduced graphene oxide. In addition, it was found that the presence of TiO_2-reduced graphene oxide decreased the concentration of dissolved O_3 and improved H_2O_2 generation, and these effects were attributed to the amount of substrate coverage on the TiO_2-reduced graphene oxide and the photodecomposition influence on the combination system.

The interaction between the pH and ZnO/α-Fe_2O_3 composite catalyst loading on amoxicillin removal were found to be significant as reported in Ansari et al. (2020). The findings suggest that the original pH and the presence of the composite catalyst in amoxicillin solution were clearly correlated with amoxicillin removal. However, the influence of pH on amoxicillin removal was relatively weaker compared to the effect of ZnO/α-Fe_2O_3 loading. Amoxicillin removal increased from approximately 80 to 90% with a decrease in the pH value from 6.6 to 4.2 as the catalyst dosage was kept at 300 mg L^{-1}. It appears that for the catalyst, an acidic solution pH was more favorable for amoxicillin removal than a basic pH, and this was presumably because the catalyst surface charge became more positive in the acidic pH range (Liu et al., 2015). Removal of levofloxacin, a quinolone antibiotic, from an aqueous solution by the method of dropping film DBD plasma combined with the Ag_3PO_4-loaded activated carbon fiber catalyst was examined (Gong et al., 2020). The findings showed that the removal rate of levofloxacin increased with an increasing dose of Ag_3PO_4/activated carbon fibers. The higher the catalyst dose, the larger the reaction area, which led to irradiation of more Ag_3PO_4 by UV/visible light, and subsequently to generation of additional reactive radicals and increase in the levofloxacin degradation rate. In addition, the energy yield of levofloxacin was enhanced in the presence of additional catalysts, while at a fixed catalyst dose, an increase in the energy yield was observed with an increasing levofloxacin removal rate and discharge time. At a catalyst dose of 490 mg L^{-1}, the highest energy yield of 544 mg kWh^{-1} was achieved, which reduced to 0.319 mg kWh^{-1} in the absence of catalysts (Gong et al., 2020).

2.3. Removal influenced by hybrid processes with O_3, persulfate, and adsorption

The degradation of atrazine by the application of DBD plasma in combination with ozonation was explored (Vanraes et al., 2015b). The energy yield G_{50} of the hybrid process of plasma treatment and ozonation is equal to the sum of the energy yields of both methods. Based on the degrees of G_{50}, ozonation contributes to approximately 40% of overall atrazine degradation in the combined process. The use of persulfate activated by DBD combined with microbubbles to degrade atrazine in water was examined (Wang et al., 2021). Based on the comparison of degradation efficiencies of atrazine by microbubbles/persulfate, DBD/persulfate, and DBD/microbubbles/persulfate, the order of the efficiencies was DBD/microbubbles/persulfate > DBD/persulfate > microbubbles/persulfate, suggesting that DBD/microbubbles/persulfate had a distinct synergetic effect on the contaminant degradation. The removal efficiencies of atrazine using DBD/microbubbles/persulfate, DBD/persulfate, and microbubble/persulfate processes were 90%, 75%, and 20% respectively without temperature control and 65%, 55% and 10% respectively with temperature control.

Several studied have explored the effect of adsorbents such as granular-activated carbon (GAC) and biochars on the removal of contaminants during the DBD treatment process (Tang et al., 2012, 2018a; Lou et al., 2021). The degradation rate of phenol during DBD treatment appeared to increase and decrease, depending on the GAC moisture content, for a reaction time of 100 min (Tang et al., 2018a). For a GAC moisture content of 20, 35, and 10%, the degradation rate of phenol was 93.3%, 92.5%, and 91.0%, respectively. This finding can be ascribed to the fact that water molecules in the discharge area influenced the production of active species, such as $OH^{\bullet}$ and H_2O_2, by irritating and dissociating these species from the water molecules on GAC (Locke and Thagard, 2012). However, too much water content on GAC could trap electrons and decrease the production of active substances (Sun et al., 1999), thus diminishing the oxidative capacity and lowering the rate of degradation of organic chemicals. Therefore, it is concluded that increasing the water content of GAC within an acceptable range fosters the generation of reactive oxygen species for the removal of organic compounds (Tang et al., 2018a). A separate study has reported that among clean, saturated, and three different DBD regeneration cycle of GACs for bisphenol A degradation, the isotherms of DBD-treated samples changed down and the adsorption capacity was reduced to 94, 84, and 80%, respectively, with an increasing DBD regeneration cycle (Tang et al., 2012). However, the regeneration rates of the three cycles were still greater than that of the saturated one, indicating that the adsorption capability of GAC for bisphenol A was efficiently remediated by the DBD process.

2.4. Removal of various types of EDCs and PPCPs

2.4.1. Selected EDCs: hormone, pesticide/herbicides/insecticide/biocide, phenol, and plasticizer

Hormones: E2 and bisphenol A are widely known EDCs (Snyder et al., 2003). Findings about the removal of various EDCs (E1, E2, and bisphenol A) demonstrate that air plasma can effectively remove some EDCs, yielding degradation rates of 94% ($k = 0.189$ min^{-1}) for BPA, 87% ($k = 0.149$ min^{-1}) for E2, and 84% ($k = 0.132$ min^{-1}) for E1 for a reaction of 15 min at 80 kV (Sarangapani et al., 2017a). It has been commonly known that the chemical structure of a compound is the main parameter that determines its degradation as it affects the chemical persistence during the degradation process (Bai et al., 2009). The removal performances of E1 and E2 were somewhat comparable owing to their similar chemical structures. A slightly higher removal rate was achieved for bisphenol A, presumably owing to the successful production of substantial amounts of active species. The active species produced during an NTP process could favor the damage of specific reaction sites such as activated aromatic acids, C═C double bonds, and non-protonated amines (Boyd et al., 2004). In particular, this is due to the donation of e^- by –OH to the benzene ring, which activates the aromatic compounds and accelerates oxidative stress by O_3 (Boyd et al., 2004). The degradation of E1, E2, and bisphenol A appeared to be higher inside the discharge zone containing all the main reactive species than in the remote regions where mostly meta-stables existed (Sarangapani et al., 2017a). In another study, EDC degradation appeared to occur with contact with either the plasma discharge or afterglow (Sarangapani et al., 2017b).

Pesticide/herbicides/insecticide/biocide: Approximately 1,800,000 kg of *N*,*N*-diethyl-m-toluamide are used per year in the United States, with only 20% absorbed by the skin, metabolized, and excreted, indicating that the greater percentage of *N*,*N*-diethyl-m-toluamide is washed away and transferred to the water system via WW effluents (Sudakin and Trevathan, 2003). Yu et al. examined the removal practicability of an insecticide (N, *N*-diethyl-m-toluamide) in water by the method of water falling film DBD plasma under three different operating modes, viz.: M1 = no *N*,*N*-diethyl-m-toluamide + gas; M2 = *N*,*N*-diethyl-m-toluamide + no gas; M3 = *N*,*N*-diethyl-m-toluamide + gas (Yu et al., 2017). *N*, *N*-diethyl-m-toluamide degradation as a function of reaction time under the three operating conditions showed that the degradation rate of *N*, *N*-diethyl-m-toluamide in M1 was significantly low (only 6%), with a reaction time of 27 min, whereas the degradation rate of *N*,*N*-diethyl-m-toluamide in M2 and M3 was 72 and 77%, respectively, under identical treatment conditions. The pseudo-first-order rate constants (k) marginally increased from 0.047 min^{-1} (M2) to 0.053 min^{-1} (M3) after bubbling gas into *N*,*N*-diethyl-m-toluamide solution, while the k value of M1 was only 0.002 min^{-1}. The use of gas alone could not provide effective degradation of *N*,*N*-diethyl-m-toluamide. In addition, a synergy effect on the degradation was observed when *N*,

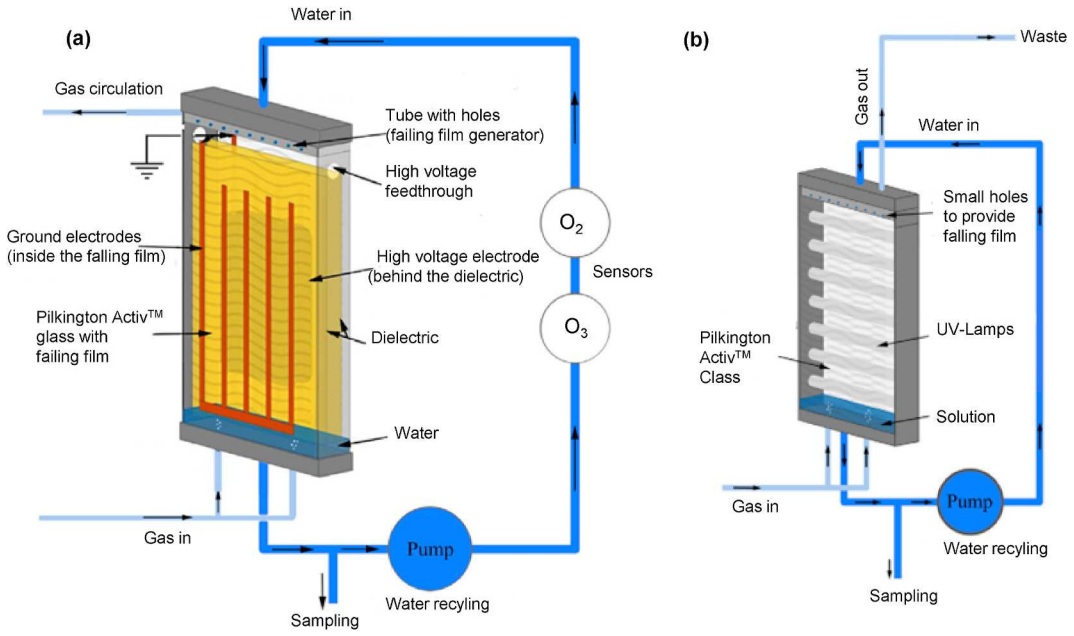

Fig. 4. Schematic diagram of (a) DBD rector and (b) photocatalytic reactor (Aziz et al., 2017).

N-diethyl-m-toluamide solution flowed through the discharge area and the gas in the discharge area was bubbled into *N*,*N*-diethyl-m-toluamide simultaneously (Yu et al., 2017).

Acute toxicity assessments were performed to estimate the influence of treated triclocarban solution on the bacterium *P. phosphoreum* T3 (Wang et al., 2016a). A greater relative inhibition rate indicated a poorer influence (Snyder and O'Connor, 2013). The relative inhibition rate of triclocarban solution without DBD treatment was 64%, while the relative inhibition rate marginally decreased to 62% for a reaction time of 30 min in a single DBD system. The relative inhibition rate declined significantly to 32% after 30-min treatment in a DBD/TiO_2-coated activated carbon fiber system. As an antibacterial agent (Chen et al., 2014), triclocarban (10 mg L^{-1}) had a 64% relative inhibition rate, indicating that its presence in solution could endanger aquatic microbes. Chlorinated by-products of DBD triclocarban degradation systems were incompletely decomposed at low mineralization levels of the system (Snyder et al., 2011), which resulted in a minor change in the relative inhibition rate of triclocarban solution after a 30-min reaction time. The 32% reduction in the relative inhibition rate can be mainly attributed to the reduction in mineralization efficiency in the DBD/TiO_2-coated activated carbon fiber system. The finding suggests that the synergetic removal of triclocarban by DBD and TiO_2-coated activated carbon fiber catalysts has a significant capacity to decrease the acute toxicity of triclocarban solution, which offers an effective and reliable method for triclocarban removal in water (Wang et al., 2016a).

Phenol: Phenol is one of main organic chemicals found in various industrial WWs, and is on the list of important contaminants published by the United States, Asia, and the European Union, owing to its great toxicity in the environment [1]. The efficiencies of phenol degradation by three different processes incorporated with TiO_2 nanotube films were compared; the processes were: (i) single-discharge in the absence of TiO_2 nanotubes (SDO), (ii) TiO_2 nanotube films spread over the surface of a discharge reactor cylinder (TSD), and (iii) TiO_2 nanotube films attached to a stainless steel electrode surface (TAD) in a discharge process (Zhang et al., 2013). The generated H_2O_2 concentration levels were 126, 154, and 173 mg L^{-1} for a discharge contact time of 30 min at 16 kV in the SDO, TAD, and TSD processes, respectively. In addition, the observed findings showed that the photocatalysis of the TiO_2 nanotubes was more distinctive in the TiO_2–plasma combination processes compared with the SDO process, particularly in the TSD process. For the TiO_2–plasma combination processes, the amount of H_2O_2 produced in the TSD process was greater than that produced in the TAD process. This finding may be attributed to the fact that the TiO_2 nanotube films were very stable in the TSD system and, thus, the synergistic impact of the TiO_2 photocatalyst and the plasma improved compared to their synergistic impact in the TAD system (Zhang et al., 2013). O_3 is one of the most significant active species generated in a discharge system that contains O_2 (Lukes et al., 2005). The rate of O_3 production in solution increased with an increasing discharge input voltage in both the single discharge and TiO_2 nanotubes–plasma combination processes. Unlike the pulsed discharge SDO process, the produced O_3 amounts were relatively small in both combination processes, with that in the TSD process the smaller (Zhang et al., 2013).

Plasticizer: Bisphenol A is widely known as one of the most common EDCs with estrogenic mimetic effects, and is usually used as an intermediate in the fabrication of various plastics and resins (Xu et al., 2014). The removal of bisphenol A by glow discharge plasma treatment (~99%) was much greater in NaCl solution than in Na_2SO_4 solution (~65%), since the generation rate of H_2O_2 in NaCl solution was approximately 50% of that in Na_2SO_4 solution (Wang et al., 2008). Both the bisphenol A degradation and H_2O_2 formation rates decreased in the presence of methanol due to its reactivity as an $OH^{\bullet}$ scavenger, suggesting that $OH^{\bullet}$ is the oxidant most responsible for bisphenol A removal and a precursor of H_2O_2. Fe^{3+} ions exhibited superior catalytic influence than Fe^{2+} ions; this result is inconsistent with the theories of the Fenton reaction as the degree of the reaction of Fe^{3+} ion and H_2O_2 is much smaller than that of Fe^{2+}ion and H_2O_2. Once aqueous bisphenol comes in contact with the glow discharge plasma, it first reacts with $OH^{\bullet}$ to produce intermediates, such as 2,2-bis(4-hydroxyphenyl)propanol, 2, 2-bis(4-hydroxyphenyl) propanal, 2,2-bis(4-hydroxyphenyl)propanoic acid, and 2-(4hydroxylphenyl)-2-(3,4-dihydroxyphenyl)propane, through H abstraction or electrophilic addition to the benzene ring of bisphenol A (Vonsonntag and Schuchmann, 1991). Dissolved organic carbon (DOC) of the solution slowly decreased with increasing reaction time, while, without catalysts, the solution chemical oxygen demand was enhanced with increasing reaction time and sharply declined with the addition of iron salts (Wang et al., 2008). Since UV irradiation is one of the main sources of DBD energy release, its role in the removal of bisphenol A was clearly studied (Zhang et al., 2016). The degradation rates of bisphenol A increased by 31 and 15% with the addition of 30

mM H_2O_2 in bisphenol A solution irradiated by UV light from argon–DBD and air–DBD, respectively. These findings clearly indicate that external H_2O_2 could improve the degradation rate of bisphenol A by UV irradiation from DBD.

2.4.2. Selected PPCPs-I: analgesic, antianxiety, and antibiotic

Analgesic: It is important to evaluate the effectiveness of the NTP process compared to other advanced oxidation processes. The performance of DBD treatment based on the degradation of two non-steroidal anti-inflammatory PhACs (diclofenac and ibuprofen) was compared with the performances of ozonation, photocatalytic ozonation, and photocatalytic oxidation with TiO_2 (Aziz et al., 2017). A schematic diagram is described for both the DBD and photocatalytic reactors in Fig. 4. The removal of diclofenac and ibuprofen by ozonation and photocatalytic ozonation indicated that direct attack of the PhACs by O_3 in the dark condition was anticipated to be the primary removal mechanism owing to the pH of the original solutions employed (pH 5.6) (Moreira et al., 2015). While the reaction of $OH^•$ with each of diclofenac and ibuprofen was very rapid, the reaction of O_3 with diclofenac was much quicker than the reaction with ibuprofen. Thus, direct ozonation led to very rapid removal of diclofenac, which was totally degraded in a contact time of 4 min. In addition, the presence of two chlorine atoms in the aromatic ring of diclofenac caused rapid dechlorination by ozonation and, therefore, an improvement in diclofenac removal efficiency (Pera-Titus et al., 2004). An O_3–UV combination process showed only a minimal impact on the removal of diclofenac. In contrast, DOC degradation by photocatalytic ozonation was much quicker than by direct ozonation in the dark condition. The removal of ibuprofen at pH = 5.7 by direct ozonation was lower than that of diclofenac. Photocatalytic ozonation improved the removal of ibuprofen, mainly due to the oxidation of ibuprofen by the produced $OH^•$, either through O_3 photolysis or photocatalysis of O_3 molecules by photo-produced e^- on the TiO_2 coating on the surface of Pilkington™ active glass (Piera et al., 2000). However, the photocatalytic oxidation (TiO_2/O_2/UV) of both compounds was somewhat mild, owing to the lower rate of $OH^•$ generation in aqueous solution by only little heterogeneous reactions on TiO_2 (Mehrjouei et al., 2014).

In general, advanced oxidation processes have been widely known to effectively remove PhACs, and it is assumed that the degradation byproducts are rather less toxic and more biodegradable (Brillas, 2020). The toxicity of ibuprofen intermediates obtained during ibuprofen degradation by DBD treatment was evaluated using the bioassays of *Vibrio fischeri* and *Artemia salina* (Markovic et al., 2015). The reported ibuprofen EC_{50} (half maximum effective concentration)/LC_{50} (half lethal concentration) value for V. fischeri was 19.1 mg L^{-1} (Ferre and Ridoux, 2001). While in the Fe^{2+} treatment only the toxicity impact index TII50 of ibuprofen was high, leading to its being regarded as toxic, several degradation byproducts obtained were very similar to those obtained in the DBD and DBD/Fenton treatments (Markovic et al., 2015). Nevertheless, the DBD and DBD/Fenton treatments appeared to lack of toxicity impact. This is presumably due to the presence of a very strong and nonselective oxidizer, such as $OH^•$, which can effectively decrease the original amount of numerous contaminants (Magureanu et al., 2010). Additionally, both reactive species (O_3 and H_2O_2) produced during the DBD process can react with contaminants outside the reactor (Dojcinovic et al., 2011) and provide somewhat less toxic intermediates and final products during long degradation of aromatic structures. In addition, H_2O_2 produced within the reactor in the presence of a catalyst can improve the total oxidizing capacity through the Fenton reaction and increase the rate of plasma treatment (Bubnov et al., 2006).

Antianxiety: A pilot-scale NTP advanced oxidation process showed that the comparative removal efficiencies of serval PhACs were very similar to those of the batch test (Gerrity et al., 2010). For instance, carbamazepine and trimethoprim exhibited the fastest removal, while primidone and meprobamate were the most difficult contaminants to degrade. At the maximum degree of energy utilization (1.8 kWh m^{-3}), each contaminant except meprobamate had no less than 70% removal. The removal of trimethoprim could not be assessed because of its low initial ambient concentration in the WW. Electrical energy per order values for the less degradable contaminants (meprobamate and primidone) reduced by 64 and 42%, respectively, as the energy utilization increased from 0.7 to 1.8 kWh m^3. Electrical energy per order values for dilantin and atenolol declined by nearly 20% over a similar range of energy consumption. The electrical energy per order values for the most sensitive contaminants (carbamazepine and trimethoprim) essentially improved by 38 and > 99%, respectively, owing to their fast removal at minimal rates of energy consumption. Most contaminants were distinguished by electrical energy per order values ranging from 1 to 5 kWh m^3-log, while meprobamate needed 13–14 kWh m^3-log with one reactor in the process. Generally, the single-pass WW test was more effective than the batch test for obtaining the electrical energy per order values, owing to the O_3 oxidant at the start of each separate scenario, which gave a more suitable description of the real treatment circumstances (Gerrity et al., 2010).

Antibiotic: The antibiotics, ofloxacin and ciprofloxacin, are commonly found in aquatic environment (Kovalakova et al., 2020). As previously described in detail, a DBD process produces various oxidizing species, such as $OH^•$, $H^•$, O_3, and H_2O_2, of which $OH^•$ is regarded as a very powerful non-selective oxidant (E_o = 2.85 V/SHE) (Locke and Thagard, 2012). While the removal rate of ciprofloxacin and ofloxacin in deionized synthetic water was 88 and 91%, respectively, the addition of the tertiary butyl alcohol at a concentration of 4 mmol L^{-1} decreased the degradation efficiency of these contaminants to 66% for ciprofloxacin and 72% for ofloxacin due to its scavenging behavior (Sarangapani et al., 2019). The reaction of the $OH^•$ with most organic chemicals appears to be either by H abstraction with saturated aliphatic hydrocarbons/alcohols, or the addition of electrophilic unsaturated hydrocarbons (Piskarev et al., 2018). However it was interesting to observe greater degradation rates in the presence of CCl_4 due to its promoting behavior by quacking $H^•$ in water; 90.5% for ciprofloxacin and 93% for ofloxacin (Sarangapani et al., 2019). This result could be ascribed to a decrease in $H^•$ concentration, which prevents the degree of recombination between $OH^•$ and $H^•$ (Wang et al., 2017a). Magureanu et al. reported that almost all identified byproducts of the degradation of the antibiotics, amoxicillin, ampicillin, and oxacillin, by DBD treatment resulted from hydrolysis, decarboxylation, or soft oxidation (Magureanu et al., 2011).

A study on the removal of the sulfonamide antibiotics, sulfathiazole, sulfamethazine and sulfamethoxazole, by DBD plasma treatment found that the removal rate was much faster with O_2 than that with dry air for all the contaminants (Kim et al., 2015b). The antibiotics showed different reactions to the plasma treatment according to their physicochemical properties. Among the contaminants studied, it was found that sulfamethazine was the most readily degradable, while sulfamethoxazole was the most difficult to remove. As anticipated, total degradation occurred when O_2 was utilized as the operating gas for the production of plasma. Even if the plasmatic gas was introduced to the contaminant solution containing various reactive species, an assumption was made that long-lived O_3 plays a crucial role in the removal. O_3 dissolved in aqueous solution could produce $OH^•$, which is a much more powerful oxidant than O_3 itself (Staehelin et al., 1984). The oxidation potentials of $OH^•$ and O_3 are 2.80 and 2.07 V, respectively (Sun et al., 1997). The amount of O_3 produced at 20.1 kV was determined to be 5.6 mg L^{-1} for air and 14.2 mg L^{-1} for O_2 (Kim et al., 2015b). In general, a greater O_3 concentration could lead to quicker removal once the other circumstances are identical.

2.4.3. Selected PPCPs-II: anticonvulsant, antiepileptic, antihypertensive, anti-inflammatory, stimulant, surfactant, and X-ray contrast medium

Three target EDCs (the antiepileptic drug carbamazepine, the blood lipid regulator clofibric acid, and the contrast medium iopromide) were effectively removed in ultrapure water by corona discharge within a

Table 3
Summary of selected EDC and PPCP removal by (catalytic) NTP treatment.

EDC/PPCP class	C_0 (μg L^{-1})	Catalyst or hybrid	Experimental condition	Key removal or rate constant	Ref.
Analgesic					
Acetaminophen	20,000	TiO_2-reduced graphene oxide	DBD; SDW; 18–24 kV; 18 min	~45, 60, 80, & 90% at 18, 20, 22, & 24 kV, respectively	Zhang et al. (2017a)
Diclofenac	50,000	Ozonation; photocatalytic oxidation	DBD; SDW; 21 kV; 5–20 kHz; 90 min; Ar: Ar/O_2 (80:20)	>99% (30 min); DBD > ozonation	(Aziz et al., 2017, 2019)
	10,000	Ozonation; UV; TiO_2	DBD; SDW; 50 W; 10 min;	~80% w/O_3; ~90% w/O_3+UV; >99% w/O_3+UV + TiO_2	Jankunaite et al. (2017)
	500 μM	Fenton	PCP; SDW; 5.024 mW; 100 kHz; 70 min	>99% (30 min); Fenton > plasma	Banaschik et al. (2018)
Ibuprofen	50,000	Ozonation; photocatalytic oxidation	DBD; SDW; 21 kV; 5–20 kHz; 90 min; Ar: Ar/O_2 (80:20)	>99% (15 min); DBD > ozonation	(Aziz et al., 2017, 2019)
	0.1 mM		DBD; SDW; 18 kV; 25 Hz; 60 min	~75% mineralize. (higher with low input energy)	Magureanu et al. (2018)
	60,000	Fenton	DBD; SDW; 17 kV; 300 Hz; 15 min	~80% (Fenton); 99% (plasma + Fenton)	Markovic et al. (2015)
Ketoprofen	10,000	Ozonation; UV; TiO_2	DBD; SDW; 50 W; 10 min;	~80% w/O_3; >99% w/O_3+UV, O_3+UV + TiO_2	Jankunaite et al. (2017)
Naproxen	10,000–30,000		DBD; SDW; 0.1 kV; 40–80 W; 6 min	~90–99% (blank >40/120 mg L^{-1} Fe^{2+})	Wang et al. (2013)
Ofloxacin	10,000		DBD; SME; 70–80 kV; 25 min	~90% (DI); ~75–85% (meet effluent)	Sarangapani et al. (2019)
Paracetamol	25,000	Fenton	DBD; SDW; 5.9 kV; 500 Hz; 60 min	~90% (plasma only); ~95% (plasma + catalyst)	Korichi et al. (2020)
	10,000–100,000		DBD; SDW; 0–20 kHz; 500 W; 60 min	53–100% (100-10 mg L^{-1}, respectively).	Pan and Qiao (2019)
Antianxiety					
Meprobamate	0.256, 0.933		DBD; WWE/SSW; 8 kV; 500 Hz; 1.75/7.5 kWh/m^3	~90% (batch); ~60% (pilot)	Gerrity et al. (2010)
Antibiotic					
Amoxicillin	16,000	ZnO/α-Fe_2O_3	DBD; SWW; 15 kV; 50 Hz; 25 min; pH 4.5	0.198 min^{-1} (99.3%)	(Ansari et al., 220)
β-lactam (amoxicillin, oxacillin, ampicillin)	100,000		DBD; SDW; 17 kV; 50 Hz; 120 min	10–20% mineralization	Magureanu et al. (2011)
Ciprofloxacin	10,000		DBD; SME; 70–80 kV; 25 min	~80–90% (DI); ~70–85% (meet effluent)	Sarangapani et al. (2019)
	1000–10,000		PCP; SDW; 15–25 kV; 25–30 kHz; 10 min	~90–100% (increased with increasing kV and Hz)	Singh et al. (2017a)
Levofloxacin	10,000–30,000	Ag_3PO_4, activated carbon fibers	DBD; SDW; 8–14 kV; 18 min	~80–95% depending on initial conc., voltage, & circulation flowrate	Gong et al. (2020)
Norfloxacin	10,000		DBD; SDW; 0–50 kV; 40–80 W; 4 min; H_2O_2 & Fe^{2+}	~75–95% depending on H_2O_2 concentration	Xu et al. (2020)
Sulfadiazine	10,000	Fenton	DBD; SDW; 100–150 W; 30 min	~80->99% (power, C_o, pH, and Fe^{2+})	Rong et al. (2014)
Sulfathiazole, sulfamethazine, sulfamethoxazole	50,000		DBD; SDW; 3.5 kV; 60 Hz; 60 min	>99% (40 min); sulfamethazine > sulfathiazole > sulfamethoxazole	Kim et al. (2015b)
Sulfamethoxazole	50,000–100,000	ZrO_2/CeO_2	DBD; SDW; 18 kV; 50 Hz; 90 min	~90% (50 mg L^{-1}); ~65% (100 mg L^{-1})	Reddy and Subrahmanyam (2015)
Trimethoprim	0.039, 1.2		DBD; WWE/SSW; 8 kV; 500 Hz; 1.75/7.5 kWh/m^3	~70% (batch); ~60% (pilot)	Gerrity et al. (2010)
Tetracycline	50,000		Coaxial-type DBD; SDW; 16–22 kV; 100 Hz; 30 min	~75–92% (22 > 20 > 18 > 16 kV)	Hao et al. (2020)
	50,000	Biochars	DBD; SDW; 6–8 kV; 38.8 W; 5 min	~70% (6 kV); ~85% (7 kV); ~90% (8 kV);	Lou et al. (2021)
	40,000	Persulfate	DBD; SDW; 7 kV; 1.0 L min^{-1}; 15 min	87.5% (0.232 min^{-1})	Tang et al. (2018b)
	20,000		DBD; SDW; 4.8 kV; 10 kHz; 5 min	94.3% with sodium percarbonate	Tang et al. (2019)
	50,000–200,000	Natural soil particles	PCP; MWW; 0–24.1 kV; 75 Hz; 60 min	~60, 80, & 95% at 200, 100, & 34 μS^{-1}, respectively	Wang et al. (2018)
	50,000–200,000	Mn/γ-Al_2O_3	DBD; SDW; 50Hz; 1.3 W; 40 min	~65–99% (tetracycline); ~20–90% (COD)	Wang et al. (2019)
Anticonvulsant					
Dilantin	0.165, 1.005		DBD; WWE/SSW; 8 kV; 500 Hz; 7.5 kWh/m^3	~90% (SSW); ~78% (WWE)	Gerrity et al. (2010)
Primidone	0.219, 1.6		DBD; WWE/SSW; 8 kV; 500 Hz; 7.5 kWh/m^3	~90% (SSW); 80% (WWE)	Gerrity et al. (2010)

(*continued on next page*)

Table 3 (*continued*)

EDC/PPCP class	C_0 (μg L^{-1})	Catalyst or hybrid	Experimental condition	Key removal or rate constant	Ref.
Antiepileptic					
Carbamazepine	65 ± 11		DBD; SWW; 40 kV; 500 Hz; 6 h	>99%	Gur-Reznik et al. (2011)
	0.219, 1.6		DBD; WWE/SSW; 8 kV; 500 Hz; 7.5 kWh/m^3	~90% (SSW); ~95% (WWE)	Gerrity et al. (2010)
	10,000	Ozonation; UV; TiO_2	DBD; SDW; 50 W; 10 min;	~65% w/O_3; 80% w/O_3+UV; >99% w/O_3+UV + TiO_2	Jankunaite et al. (2017)
	100 μM	Boron doped diamond, iron	DBD; LLWW; 25–35 kV; 30 kHz; 500 W; 30 min	~85% (15 min); ~95% (30 min)	Krause et al. (2009)
	20,000		DBD; SDW; 0.7, 12 W; 60 min	100% (*Ex situ*); 91% (*In situ*)	Liu et al. (2012b)
Antihypertensive					
Verapamil	0.1–0.5 mM		DBD; SDW; 18 kV; 50 Hz; N_2:O_2 (80:20); 180 min	>99% (40 min, 0.1 mM); >99% (90 min, 0.5 mM);	Krishna et al. (2016)
Antiinflammatory					
Pentoxifylline	25,000–150,000		DBD; SDW; 12 kV; 120 Hz; 80 min	34–130 × 10^{-3} min^{-1}; $t_{1/2}$ = 5.3–20.6 min	Magureanu et al. (2010)
Hormone/steroid					
17β-Estradiol (E2), estrone (E1)	2000		DBD; MDE; 60–80 kV; 50 Hz; 15 min	~40% (60 kV); ~60% (60 kV); ~80% (60 kV);	Sarangapani et al. (2017a)
17α-ethinyl estradiol (EE2)	200		DBD; SDW; 40 W; water flow rate = 56.3 mL min^{-1}; 30 min	99.6% at 2.42 kWh m^3	Wardenier et al. (2019)
Fluocinolone acetonide, clobetasol propionate	0.02–5 mM		SDW/NSW/WWE; DBD; 0–60 kV; 35.9–58.2 W; 120 min	80–83% with increasing power	Liu et al. (2019)
Pesticide/herbicide/insecticide/biocide					
Atrazine	21,600		DBD; SDW; 25 kV; 120 W; 14 min	>95% (Fe^{2+}); 40–60% (isopropyl alcohol or Na_2CO_3)	Feng et al. (2016)
	1000–5000		DBD; SDW; 12 kV; 94 kHz; 24 W; 90 min	>99% (30 min, Reactor 1; 45 min, Reactor 2)	Hijosa-Valsero et al. (2013)
	30	Ozonation, activated carbon	DBD; SDW; 6.0–7.5 kV; 35.7 Hz; 20–25 W; 20 min	~95% (plasma + O_3); ~90% (plasma); ~70% (O_3)	Vanraes et al. (2015b)
	50,000	Microbubbles	DBD; SDW; 65–105 W; 75 min	~20, 60, & 80–90% at 105 w/o persulfate, 65, & 80–90%, respectively	Wang et al. (2021)
Carbofuran	1000–10,000		PCP; NSW; 23 kV; 25 kHz; 58.7 W; 40 min	>99% (10 mL min^{-1}); ~70% (40 mL min^{-1})	Singh et al. (2019)
Chlorfenvinfos	1000–5000		DBD; SDW; 12 kV; 94 kHz; 24 W; 90 min	>99% (10 min, Reactor 1; 20 min, Reactor 2)	Hijosa-Valsero et al. (2013)
DEET	10,000		DBD; SDW; 12–18 kV; 0–30 kHz; 27 min	~50% (100 mL min^{-1}); ~75% (160 mL min^{-1}); ~80% (250 mL min^{-1})	Yu et al. (2017)
Irgarol 1051	0.1 mmol L^{-1}	TiO_2	DBD; SDW; 18 kV; 50 Hz; 2.6 W; 50–240 min	~50–99% (23 > 56 > 100 > 200 > no TiO_2 mg L^{-1})	Giardina et al. (2018)
Tributyltin	10,000		DBD; SDW; 20 kV; 100 kHz; 30 W; 22 min	>95% (5 min)	Hijosa-Valsero et al. (2014)
Triclocarban	10,000	TiO_2 coated activated carbon fibers	DBD; SDW; 38 W; 30 min	~20, 35, 70, & 90% with Ar, N_2, air, & O_2, respectively	Wang et al. (2016a)
Phenol					
Phenol	0.055 mmol L^{-1}		DBD/STR; SDW; 16 kV; 12–18 kHz; N_2:O_2 (80:20)	>95% (at >4000 J) DBD; >95% (at >1750 J) DBD;	Bosi et al. (2018)
	0.1–0.01 mmol L^{-1}		DBD; SDW; 16.5–18 kV; 50 Hz; 240 min	91% (~15% CO_2), DI water; 93% (~45% CO_2), phosphate buffer	Ceriani et al. (2018)
	100,000	TiO_2, Fe^{3+}	PCP; SDW; 20 kV; 50 Hz; 9 W 120 min	49% (plasma); 57% (plasma/TiO_2); 585 (plasma/Fe^{3+}); 70% (plasma/TiO_2/Fe^{3+})	Duan et al. (2018)
	100,000	TiO_2	PDD; SDW; 0–40 kV; 1.42 kHz; 40 min	~80–90% (8 kV > 15.8 kV); ~90–99% (TiO_2)	Jianjin et al. (2015)
	5,000,000	GAC	PDD; SDW; 18–28 kV; 50 Hz; 100 min	~90% (28 kV); ~85% (23 kV); ~80% (18 kV);	Tang et al. (2018a)
	20,000–60,000	Fe-based zeolite	DBD; SDW; 20 kV; 14.5 kHz; 20 min; 2.0 g Fe-zeolite	~10–20% (plasma); ~25–55% (plasma + Fe-zeolite)	Wu et al. (2020)
	50,000	TiO_2	PCP; SDW; 12–16 kV; 100 Hz; 30 min	0.04–0.12 min-1; enhanced effect = 1–2.8	Zhang et al. (2013)

(*continued on next page*)

Table 3 (*continued*)

EDC/PPCP class	C_0 (μg L^{-1})	Catalyst or hybrid	Experimental condition	Key removal or rate constant	Ref.
2,4-dibromophenol	1000–5000		DBD; SDW; 12 kV; 94 kHz; 24 W; 90 min	>99% (15 min, Reactor 1; 40 min, Reactor 2)	Hijosa-Valsero et al. (2013)
Plasticizer					
Bisphenol A	1000		DBD; SDW; 20 kV; 100 kHz; 30 W; 22 min	>95% (5 min)	Hijosa-Valsero et al. (2014)
	2000		DBD; MDE; 60–80 kV; 50 Hz; 15 min	~45% (60 kV); ~70% (60 kV); ~90% (60 kV);	Sarangapani et al. (2017a)
	50,000	GAC	DBD; SDW; 15–27 kV; 50 Hz; 50 min	~60–85% (15–27 kV)	Tang et al. (2012)
	100,000		DBD; SDW; 0.5 kV; 60 min	~>95% (NaCl); ~55–65% (Na_2PO_4 or Na_2SO_4)	Wang et al. (2008)
	50,000	UV	DBD; SDW; 20 kV; 5–25 kHz; 10 min	~>95% (DBD in air); ~<10% (UV from DBD)	Zhang et al. (2016)
Stimulant					
Caffeine	1000 100,000		DBD; SDW; 60 W, 10 kHz, 4 min	96.6% 72.6%	Al Bratty et al. (2021)
Surfactant					
Perfluorooctanoic acid	20,000	Fe_3O_4@SiO_2–BiOBr	DBD; SDW; 22 kV; 60 min	74% (plasma only); 93% (plasma + catalyst)	Wang et al. (2017b)
X-ray contrast medium					
Diatrizoate	200, 10,000		PCP; SDW; 11 kV; 3 kHz; 60 min	~90% (O_2 plasma); ~40% (air plasma)	Puertas et al. (2021)
Iopromide, diatrizoate	65 ± 11		DBD; SWW; 40 kV; 500 Hz; 6 h	25->99% (diatrizoate) >99% (iopromide)	Gur-Reznik et al. (2011)
Iopromide	100 μM	Boron doped diamond, iron	DBD; LLWW; 25–35 kV; 30 kHz; 500 W; 30 min	~90% (15 min); ~95% (30 min)	Krause et al. (2009)

C_0 = EDC or PPCP initial concentration; BOD = biochemical oxygen demand; GAC = granular activated carbon; COD = chemical oxygen demand; DBD = dielectric barrier discharge; DEET = N, *N*-Diethyl-meta-toluamide LLWW = landfill leachate wastewater; MDE = model dairy effluent; MWW = municipal wastewater; NSW = natural surface water; PCP = pulsed corona plasma; PDD = pulsed diaphragm discharge; SDW = synthetic drinking water; SME = synthetic meet effluent; SSW = spiked surface water; STR = pin-to-plate streamer; SWW = synthetic wastewater; UV = ultraviolet; w/= with; w/o = without; WWE = wastewater effluent.

treatment time of 0.5 h; the treatment showed >99% removal for iopromide, 99% removal for clofibric acid, and 98% removal for carbamazepine (Krause et al., 2009). However, approximately 15–25% lower degradation of these contaminants was observed with landfill leachate, which contains much more inorganics and organics than ultrapure water, WW effluents, and surface waters. The effect of the counter electrode materials (boron-doped diamond, titanium, iridium oxide, and iron) on the removal efficiency showed that the degradation rates varied significantly depending on these materials. Carbamazepine removal of 98, 89, 84, and 64% was observed in the presence of the boron-doped diamond, titanium, iridium oxide, and iron electrodes, respectively. The degradation of carbamazepine was quicker in the presence of the boron-doped diamond electrode compared to the other electrodes. This might be linked to the O_2 evolution potential of the electrode materials. The boron-doped diamond and iridium oxide electrodes have O_2 evolution potentials of 2.3 and 1.6 V, respectively, with respect to the normal hydrogen electrode (Chen, 2004). A low O_2 evolution potential can be anticipated to reduce the reaction rate, owing to the generation of O_2 as opposed to the removal of the target contaminants (Krause et al., 2009). In a separate study, there was 100% carbamazepine degradation after 3-min contact with the *ex situ* electric discharge on the water surface, while the *in situ* discharge only degraded 81% of the carbamazepine after 60 min (Liu et al., 2012b).

Antihypertensive verapamil used to treat cardiovascular disorders was successfully degraded by air NTP in a DBD reactor (Krishna et al., 2016). The findings showed that the majority of the byproducts were as a result of the reaction of verapamil with O_3, which was one of the dominant oxidizing species. A small number of intermediates were identified presumably due to direct attack by $OH^{\bullet}$, although the production of any intermediates due to reaction with reactive nitrogen species could not be proved. In a separate study, after 1 h of DBD treatment, 92% degradation of anti-inflammatory pentoxifylline (C_o = 100,000 μg L^{-1}) was observed, which was equivalent to a degradation yield of 16 g kWh^{-1} (Magureanu et al., 2010). In addition, pentoxifylline degradation increased at a quicker rate with decreasing initial concentrations (in the range of 25,000 to 150,000 μg/L), with a rate constant of 13.0×10^{-2} min^{-1} at 25,000 μg/L and 3.37×10^{-2} min^{-1} at 150,000 μg/L. Al Bratty et al. reported that a very high degradation rate of caffeine in aqueous solution (96.6%) was achieved at an initial concentration of 1 mg L^{-1} during DBD treatment without catalysts, expensive gases, and organic solvents (Al Bratty et al., 2021). Based on current literature, Table 3 summarizes the degradation rates of selected EDCs and PPCPs during NTP treatment for different initial concentrations, catalyst types, discharge conditions, source water types, and reaction times.

2.5. Mineralization, pathway, and degradation mechanism of selected EDCs/PPCPs

The various reactive oxidants produced during NTP processes could result in significant oxidation and mineralization of organic compounds, and break these compounds down to CO_2, H_2O, and different mineral acids (Ansari et al., 2021). The removal of three target compounds spiked dairy effluent corresponds to dissolved organic carbon (DOC) concentrations (C_o = 1130–1250 mg L^{-1} for bisphenol A, E1, and E2) linearly increased with increasing reaction time, with a maximum degradation of approximately 18–22% after 15 min of an NTP process (Sarangapani et al., 2017b). While all the target compounds were successfully removed (>80%) within 15 min, less than 30% of the compounds were removed based on their DOC, which could be ascribed to the production of relatively small compounds such as $C_2H_2O_4$ and CH_2O_2 prior to the mineralization of the entire compounds (Kim et al.,

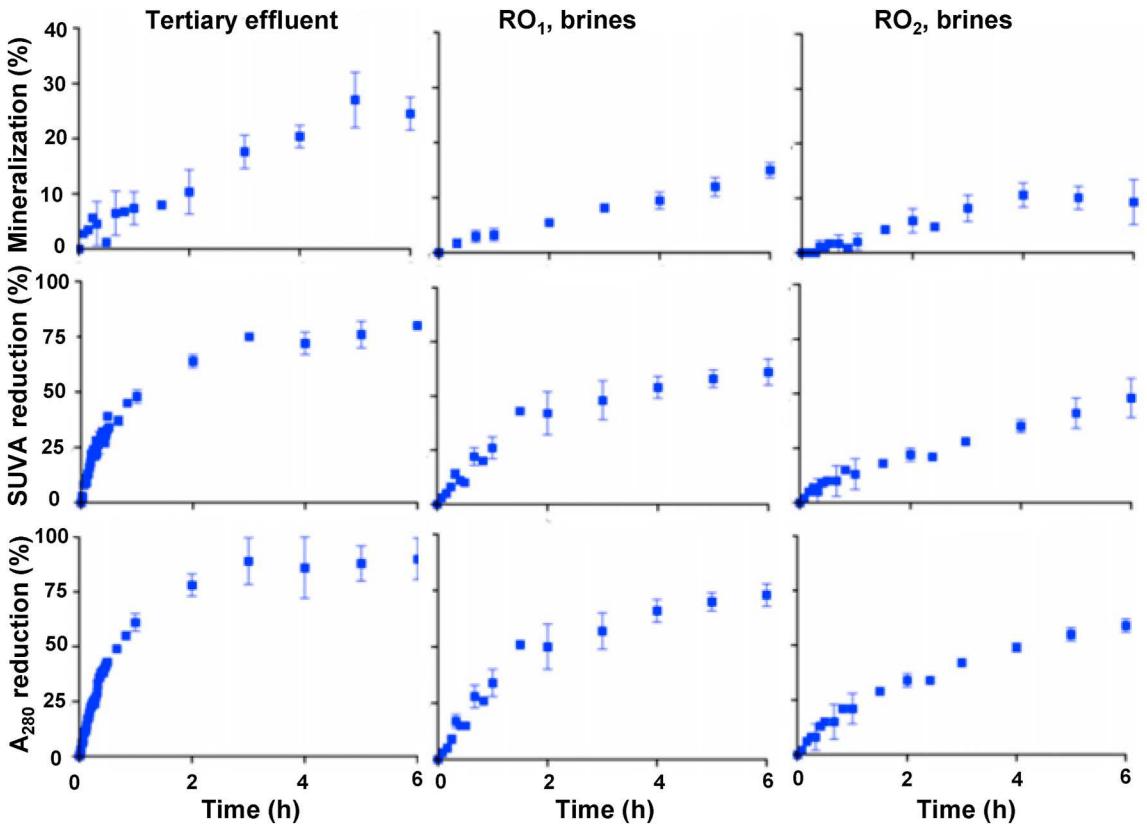

Fig. 5. Fate of dissolved organic matter background upon NTP treatment in different waters (tertiary effluent and reverse osmosis (RO) brines). Upper panel: dissolved organic carbon (DOC) mineralization profiles; middle panel: specific UV absorbance (SUVA) reduction profiles; lower panel: change in absorbance at 280 nm (A280). Values represent average ± standard deviation of 3–5 independent replicates (Gur-Reznik et al., 2011).

2015b). With an initial concentration of 10 mg L^{-1} for various PhACs (diclofenac, carbamazepine, ciprofloxacin, and carbofuran), a considerable decrease in DOC was achieved, reaching approximately 70% (5.93–1.8 mg L^{-1}), 65% (7.22–2.53 mg L^{-1}) and 50% (11.3–5.64 mg L^{-1}) in deionized water, lake water, and river water, respectively during plasma treatment (Singh et al., 2019). The reduction in DOC with increasing reaction time suggested that most of the contaminants were mineralized to carbon dioxide, water, and nitrate. Numerous byproduts/intermediates of all the contaminants during the plasma treatment process have been well described in previous studies (Tian et al., 2013; Singh et al., 2017a). While an assumption was made that the remaining DOC in treated water could provide various levels of toxicity, the toxicity test verified that the toxic behavior of the contaminants was entirely eliminated in deionized water and lake water after the plasma treatment (Singh et al., 2019).

The fate of iodinated contrast medium (iopromide) during DBD treatment is described in Fig. 5 based on mineralization associated with DOC, specific UVA (UVA/DOC), and UVA_{280} in different waters (tertiary effluent and reverse osmosis brines) (Gur-Reznik et al., 2011). The efficiency of DOC mineralization was approximately 25, 15, and 10% for the tertiary effluent, reverse osmosis brine 1, and reverse osmosis brine 2, respectively. Compared to mineralization, a relatively high specific UVA reduction was achieved—80, 61, and 48% for tertiary effluent, reverse osmosis brine 1, and reverse osmosis brine 2, respectively—describing substantial removal of the total DOC aromaticity (Jarusutthirak et al., 2002). A separate study also showed that the degradation of hydrophobic organic compounds based on UVA_{254} was higher than that based on DOC (Westerhoff et al., 2009). Since specific UVA is determined based on the ratio of UVA at 254 nm to DOC, this result is corroborated by the findings described here as well. UVA_{254} suggests positive oxidation of unsaturated carbon bonds (Westerhoff et al., 2009). In addition, a significant decrease based on UVA at 280 nm was also achieved 90, 73, and 59% for tertiary effluent, reverse osmosis brine 1, and reverse osmosis brine 2, respectively—which indicated that changes in the proteinic and phenolic DOC groups occurred (Gur-Reznik et al., 2011). In a separate study, the performance of iron immobilized in alginate beads as catalyst for heterogeneous electro-Fenton treatment of a malodorous compound (indole) was investigated (Ben Hammouda et al., 2016). This result provides a conclusion that indole intermediates are possibly recalcitrant to the treatment. In addition, the observed lack of substantial effect of UV irradiation indicates its insignificant influence on ferrous ions regeneration and $OH^{\bullet}$ production. Kim et al. reported red mud-activated peroxymonosulfate process for the removal of fluoroquinolones in hospital wastewater (Kim et al., 2020). The finding suggests that due to the greater reactivity between ciprofloxacin and $SO_4^{\bullet-}$, ciprofloxacin removal was more effective than flumequine removal in the presence of humic acid.

Pathways and intermediates for the removal of diclofenac by the pulsed corona plasma process or by Fenton reactions are described in Fig. 6 (Banaschik et al., 2018). In general, the findings suggest that $OH^{\bullet}$ plays a significant role in the degradation of the original chemical and nearly all intermediates. No indication was observed for chemical reactions including reactive Cl^{-}, O_3, and NO_3^{-}. Therefore, the results are somewhat similar to those of earlier studies where phenol was employed as a model contaminant to evaluate various reactive species (Banaschik et al., 2015). Four reaction steps (A to D) primarily describe the degradation of diclofenac in Fig. 6. Presumably, attack of the benzene rings is one of the main initial reactions (Hartmann et al., 2008). This is demonstrated by the byproducts I1*, with a molecular weight variation of multiples of 16 Da, representing the production of hydroxyl/phenol groups in diclofenac. Attack of the benzene rings might take place if $OH^{\bullet}$ initially separates a H atom from C, and then a second $OH^{\bullet}$ combines

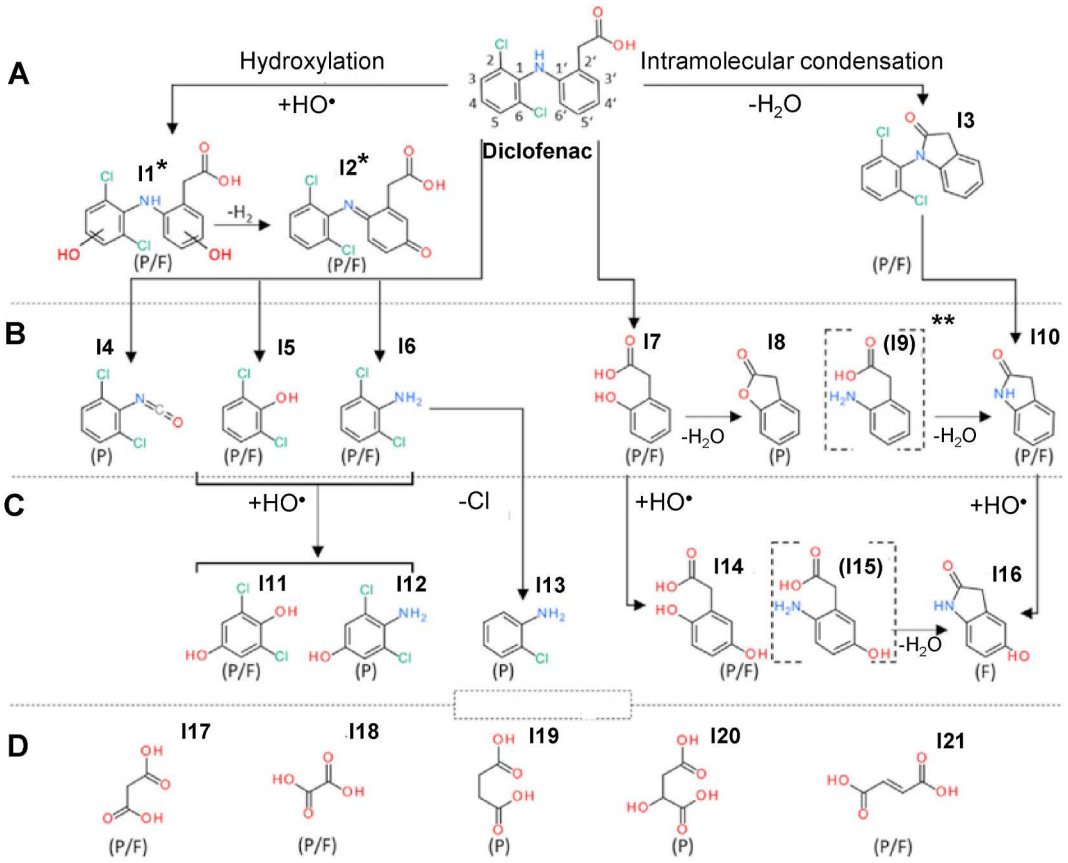

Fig. 6. Proposed degradation pathway and intermediates for the degradation of diclofenac by hydroxyl radicals formed during plasma treatment (P) or due to hydroxyl radicals generated by Fenton-processes (F). Apart from intermediates I9 and I15, all other byproducts were experimentally identified and verified. *Products were identified due to their molecular mass, physicochemical properties and description in literature (Banaschik et al., 2018).

with the C-based radical. The greatest reactive carbon atoms of the diclofenac molecule can be found in positions 4 and 4′ of the rings, while the somewhat electron-withdrawing groups, such as Cl, can also encourage reactions with carbon-4'. Additional destruction of H_2 could result in quinone-imine intermediates, such as I2* (Perez-Estrada et al., 2005). The cleavage of the C–N bond (B) leads to various characteristic derivatives (I5–I10). The diclofenac molecule is divided into two components; depending on the spatial orientation of the $OH^•$ attack, the byproduct 2,6-dichlorophenol (I5) or 2,6-dichloroaniline (I6) is produced. Their corresponding counterparts (I7 and I9) were identified as I8 and I10, owing to acidification and ring closure through solid phase extraction. It is meaningful to indicate that the cleavage byproducts of both diclofenac derivatives [(I5, I10) and (I6, I7)] could be identified, because previous studies only revealed the byproducts I6 and I7 when diclofenac was oxidized with plasma produced above the liquid (Dobrin et al., 2013). The byproduct I4 was only identified after plasma application, while a previous study also showed its generation for $OH^•$ through Fenton reactions (Beldean-Galea et al., 2014). Step C includes constant hydroxylation and dichlorination (I11–I16), which in the end (D) results in cleavage of the benzene ring structure and production of tiny organic acids (I17–I21). Thus, identical intermediates are achieved and removal pathways are comparable between plasma treatment and Fenton processes (Banaschik et al., 2018).

The degradation of atrazine during DBD treatment formed four degradation byproducts that kept the s-triazine ring with a chlorine atom (deethylatrazine and deisopropylatrazine) and two oxidized intermediates of atrazine, which were tentatively recognized as 4-chloro-6-(ethenylamino)-1,3,5-triazin-2-yl acetate and atrazine amide (Hijosa-Valsero et al., 2013). The use of DBD plasma for the degradation of atrazine from aqueous solutions exhibited no degradation byproduct (Gerrity et al., 2010). Nevertheless, the production of deethylatrazine was detected in a test using a pulsed arc electrohydraulic discharge reactor (Leitner et al., 2005). During DBD treatment combined with TiO_2-coated activated carbon fibers for triclocarban degradation, O_3 was produced from the cross-section reactions of O_2, H_2O molecules and O atom (Wang et al., 2016a). The oxidation by O_3 of organic compounds in H_2O can be described by two potential mechanisms: direct attack by O_3 and attack by $OH^•$ (Andreozzi et al., 2005). Di-hydroxy-triclocarban was identified as a byproduct based on m/z 347, suggesting that direct attack of O_3 on the aromatic benzene ring of triclocarban molecules was presumably due to generation of an aromatic hydroxyl chemical by hydroxylation (Chen et al., 2012). It was reported that the C–N bond was the highest reactive site for O_3 molecules in water (Ding et al., 2013). Therefore, the C–N bond was dissociated to produce two additional major byproducts, hydroquinone and 2-chlorohydroquinone (Wang et al., 2016a). Two potential pathways were reported at the initial stage of the oxidation reaction of acetaminophen in a plasma/TiO_2-reduced graphene oxide system (Zhang et al., 2017a). One pathway engaged with direct ozonation of acetaminophen, because O_3 attack typically continued on the aromatic rings of target compounds via production of polyhydroxy aromatics (Decoret et al., 1984). The other potential pathway was hydroxylation of acetaminophen through $OH^•$ attack on the aromatic rings (Zhang et al., 2008).

Removal of bisphenol A during NTP treatment began with phenol-moiety oxidation associated with small estrogenic activity readily attached by both $OH^•$ and $OOH^•$ (Ngundi et al., 2003). The deprotonation of bisphenol A or interaction with plasma-generated reactive species at electron-rich reaction sites occurred through $OH^•$ abstraction (Sarangapani et al., 2017a). The reaction continued by cleavage of the C–C bond, causing phenol radicals that reacted with $OH^•$ to produce

Table 4
Estimated costs comparison for various oxidation processes based on disinfection of sewage water (2010 US $/m^3) (Capodaglio, 2019).

m^3/day treated	Electron beam	Ozone	UV	Chlorine
10,000	0.29	0.25	0.17	0.013
50,000	0.073	0.086	0.171	0.013
100,000	0.050	0.064	0.054	0.013
200,000	0.041	0.053	0.047	0.013

hydroquinone/catechol and additional orthoquinone, which have fairly low estrogenic activity compared with the parent compound (bisphenol A) (Tay et al., 2012). In addition, 4-isopropenylphenol and 4-hydroxyacetophenone were produced by both direct and indirect interaction with O_3 and $OH^•$, which are somewhat comparable to intermediates found in a separate study (Ike et al., 2002). In a separate study, several intermediates were identified during the degradation of paracetamol by DBD treatment (Pan and Qiao, 2019). The production of the first intermediate (3-nitro-4-acetamidophenol) increased with the degradation of paracetamol within 5 min, decreased as the time increased, and then completely disappeared after 20 min, suggesting that 3-nitro-4-acetamidophenol might require more degradation energy than paracetamol. The production of the second intermediate (nitrosophenol) decreased after 2 min, and was undetected along with 3-nitro-4-acetamidophenol. The retention time of the third intermediate (acetamide) peak increased, and the intermediate disappeared after a contact time of 10 min, indicating that a second intermediate (*N*-methylacetamide) was formed after the production of acetamide, and its formation appeared to increase with time. It was found that paracetamol was initially oxidized to an intermediate *N*-acetyl-p-benzoquinone imine by reactive species, such as HNO_2, H_2O_2, and $OH^•$, and this intermediate then quickly reacted with HNO_2 to form 3-nitro-4-acetamidophenol (Matsuno et al., 1989). Hence, the production of 3-nitro-4-acetamidophenol occurred due to the degradation of paracetamol by air DBD plasma (Pan and Qiao, 2019).

2.6. Cost-benefit analysis

A comprehensive analysis of costs and benefits of catalytic NTP technology for the removal of EDCs and PPCPs is necessary to determine if the use of NTP is financially viable. However, there is lack of information on cost-benefit analysis with catalytic NTP treatment processes based on current studies, while Table 4 summarizes limited information on reported total cost-of-treatment evaluations for a few oxidation technologies applied to municipal wastewater disinfection (to below detection limits of pathogens) (Capodaglio, 2019). While specific cost of chlorination stays steady (the cost is largely based on chemical cost), that of other technologies reduces with increasing treated flow (owing to initial fixed costs). Among the technologies examined (electron beam, ozone, and UV), electron beam is the one with the sharpest cost decrease with increasing treated flow (Maruthi et al., 2011). While an assumption can be made that catalytic NTP technologies appear to be more effective than conventional NTP ones, it is still essential to systematically compare cost-benefit analysis between catalytic NTP and other advanced oxidation processes for the removal of EDCs and PPCPs.

3. Conclusions and areas of future research

The fate and transport of CECs, such as EDCs and PPCPs, have been widely studied in numerous water and WW treatment processes. In recent studies, NTP with and without catalysts has been observed to be effective in the degradation of various EDCs and PPCPs in aqueous solution, with the degradation efficiency significantly affected by the water quality/NTP conditions and the physicochemical properties of the contaminants/catalysts. The following general removal trends have been achieved: (i) EDC and PPCP degradation decreases with increasing solute initial concentration and in the presence of scavengers (*e.g., tert*-butanol and isopropyl alcohol), and increases with increasing input power and catalyst dose; (ii) optimal solution pH, background ions, alkalinity, NOM, temperature, gas type, gas flow rate, and catalyst type may vary depending on contaminant characteristics and the relative

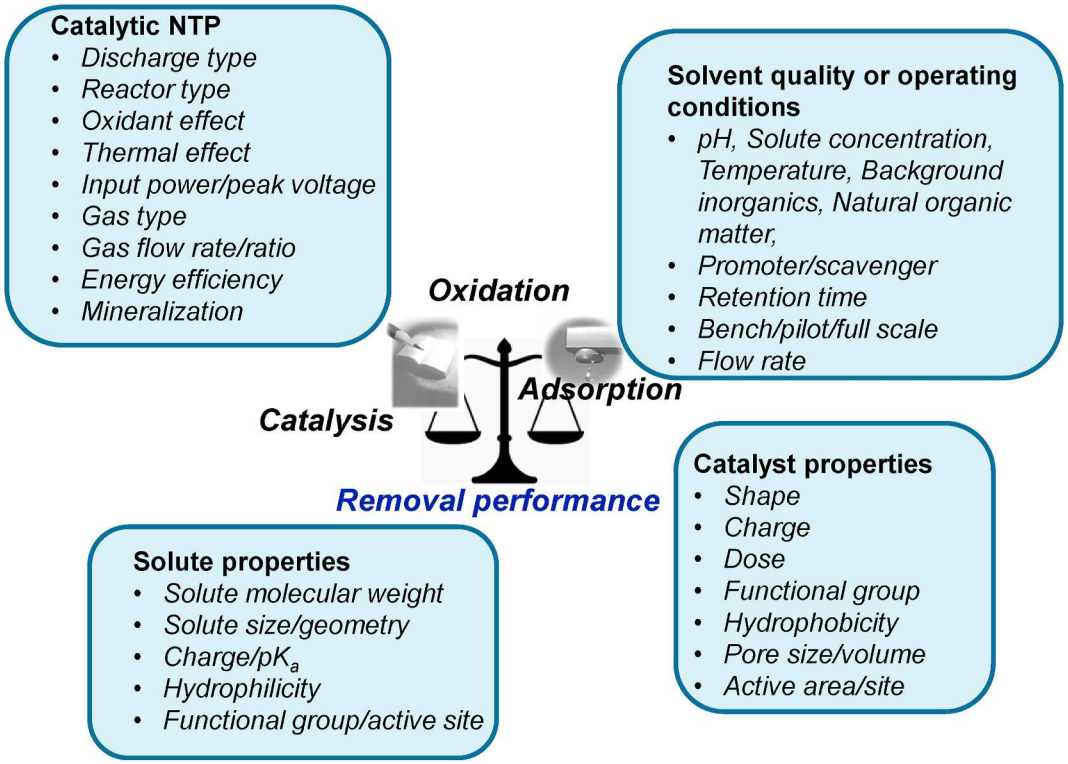

Fig. 7. Potential areas of future study of catalytic NTP systems for the removal of CECs in aqueous solution.

kinetics of reactions between the contaminants and reactive species ($OH^{\bullet}$, O_3, and $O_2^{\bullet-}$). More popular advanced oxidation processes, such as NTP/H_2O_2, UV/H_2O_2, and O_3/H_2O_2, involve substantial chemical requirement and remaining H_2O_2 quenching, which represent a considerable percentage of their operational expenses. Overall, findings in this review suggest that NTP with/without catalysts may serve as a feasible alternative to more common advanced oxidation processes, owing to its chemical-free process, *in-situ* production of reactive species, and similar energy requests for trace contaminant removal. The main advantage of the NTP advanced oxidation process is its ability to produce UV light, O_3, and $OH^{\bullet}$ without chemical supplement or UV radiation.

Nevertheless, the actual capital costs and dependability of large-scale NTP systems for water and wastewater treatment are still somewhat uncertain. In addition, since oxidation by O_3 molecules is the main removal mechanism of numerous contaminants, upcoming research needs to directly compare the performances of NTP, UV, and O_3. Such research is required prior to careful determination of the applicability of the innovative NTP technique for water and wastewater treatment. Catalysts may have a significant role in enhancing the influence of water contaminants and decreasing the operational costs of plasma catalysis. Therefore, more studies are necessary to develop various effective catalysts with superior catalytic activity. In terms of the potential practical applications of the various NTP reactors, clearly the size and the efficiency of the system are the main questions to be faced. Therefore, future development should focus on optimization of system efficiency in the design and assessment of devices to be operated on a larger scale. Furthermore, studies on the mineralization amount of original contaminants, and the production and toxicity of their byproducts need to be conducted prior to determining whether treated wastewater effluents should be utilized for water reclamation or recycling. Fig. 7 demonstrates the subjects of future studies on catalytic NTP systems in terms of catalyst/solute properties, solvent quality, operating conditions, and NTP conditions.

The novelty of this study is to review on catalytic NTP treatment for water purification: mechanisms, operation conditions, active species, and hybrid processes. In addition, this study provides a review on the removal of various contaminants such as EDCs and PPCPs in water. To the best of our knowledge, assessing the influences of different catalysts and hybrid systems on degradation provides a recent review for Chemosphere readers. These summaries of findings (over more than 200 references) would indeed be of great interest to the readership of Chemosphere for evolving in their investigation about catalytic NTP for environmental applications.

Author contributions statement

Seong-Nam Nam: Conceptualization, investigation, writing - original draft, writing - review, and editing; **Choe Earn Choong**: writing - review; **Shamia Hoque and Tanvir Farouk**: Conceptualization and review; **Jinwoo Cho and Min Jang**: review, and editing; **Shane Snyder and Michael Meadows**: Conceptualization, review, and editing; **Yeomin Yoon**: Conceptualization, supervision, project administration, and funding acquisition.

Declaration of competing interest

The authors declare that they have no known competing financial interests or personal relationships that could have appeared to influence the work reported in this paper.

Acknowledgements

This research was supported by the National Science Foundation, USA (OIA-1632824). This research was supported by Basic Science Research Program through the National Research Foundation of Korea (NRF) funded by the Ministry of Education (2021R1A6A1A03038785).

References

Al Bratty, M., Al-Rajab, A.J., Rehman, Z.U., Sharma, M., Alhazmi, H.A., Najmi, A., Muzafar, H.M.A., Javed, S.A., 2021. Fast and efficient removal of caffeine from water using dielectric barrier discharge. Appl. Water Sci. 11, 97.
Alexy, R., Kumpel, T., Kummerer, K., 2004. Assessment of degradation of 18 antibiotics in the closed bottle test. Chemosphere 57, 505–512.
Andersen, H.R., Lundsbye, M., Wedel, H.V., Eriksson, E., Ledin, A., 2007. Estrogenic personal care products in a greywater reuse system. Water Sci. Technol. 56, 45–49.
Andreozzi, R., Canterino, M., Marotta, R., Paxeus, N., 2005. Antibiotic removal from wastewaters: the ozonation of amoxicillin. J. Hazard Mater. 122, 243–250.
Ansari, M., Mahvi, A.H., Salmani, M.H., Sharifian, M., Fallahzadeh, H., Ehrampoush, M. H., 2020. Dielectric barrier discharge plasma combined with nano catalyst for aqueous amoxicillin removal: performance modeling, kinetics and optimization study, energy yield, degradation pathway, and toxicity. Separ. Purif. Technol. 251, 117270.
Ansari, M., Sharifian, M., Ehrampoush, M.H., Mahvi, A.H., Salmani, M.H., Fallahzadeh, H., 2021. Dielectric barrier discharge plasma with photocatalysts as a hybrid emerging technology for degradation of synthetic organic compounds in aqueous environments: a critical review. Chemosphere 263, 128065.
Aziz, K.H.H., Miessner, H., Mueller, S., Kalass, D., Moeller, D., Khorshid, I., Rashid, M.A. M., 2017. Degradation of pharmaceutical diclofenac and ibuprofen in aqueous solution, a direct comparison of ozonation, photocatalysis, and non-thermal plasma. Chem. Eng. J. 313, 1033–1041.
Aziz, K.H.H., Omer, K.M., Mahyar, A., Miessner, H., Mueller, S., Moeller, D., 2019. Application of photocatalytic falling film reactor to elucidate the degradation pathways of pharmaceutical diclofenac and ibuprofen in aqueous solutions. Coatings 9, 465.
Bai, Y.H., Chen, J.R., Mu, H., Zhang, C.H., Li, B.P., 2009. Reduction of dichlorvos and omethoate residues by O_2 Plasma Treatment. J. Agric. Food Chem. 57, 6238–6245.
Banaschik, R., Jablonowski, H., Bednarski, P.J., Kolb, J.F., 2018. Degradation and intermediates of diclofenac as instructive example for decomposition of recalcitrant pharmaceuticals by hydroxyl radicals generated with pulsed corona plasma in water. J. Hazard Mater. 342, 651–660.
Banaschik, R., Lukes, P., Jablonowski, H., Hammer, M.U., Weltmann, K.D., Kolb, J.F., 2015. Potential of pulsed corona discharges generated in water for the degradation of persistent pharmaceutical residues. Water Res. 84, 127–135.
Beldean-Galea, M.S., Coman, V., Copaciu, F., Thiebaut, D., Vial, J., 2014. Simultaneous identification of Fenton degradation by-products diclofenac, ibuprofen, and ketoprofen in aquatic media by comprehensive two-dimensional gas chromatography coupled with mass spectrometry. Rev. Roum. Chem. 59, 1021–1027.
Ben Hammouda, S., Fourcade, F., Assadi, A., Soutrel, I., Adhoum, N., Amrane, A., Monser, L., 2016. Effective heterogeneous electro-Fenton process for the degradation of a malodorous compound, indole, using iron loaded alginate beads as a reusable catalyst. Appl. Catal. B Environ. 182, 47–58.
Benotti, M.J., Brownawell, B.J., 2007. Distributions of pharmaceuticals in an urban estuary during both dry- and wet-weather conditions. Environ. Sci. Technol. 41, 5795–5802.
Benotti, M.J., Trenholm, R.A., Vanderford, B.J., Holady, J.C., Stanford, B.D., Snyder, S. A., 2009. Pharmaceuticals and endocrine disrupting compounds in US drinking water. Environ. Sci. Technol. 43, 597–603.
Blair, B.D., Crago, J.P., Hedman, C.J., Treguer, R.J.F., Magruder, C., Royer, L.S., Klaper, R.D., 2013. Evaluation of a model for the removal of pharmaceuticals, personal care products, and hormones from wastewater. Sci. Total Environ. 444, 515–521.
Bosi, F.J., Tampieri, F., Marotta, E., Bertani, R., Pavarin, D., Paradisi, C., 2018. Characterization and comparative evaluation of two atmospheric plasma sources for water treatment. Plasma Process. Polym. 15, 1700130.
Boyd, G.R., Palmeri, J.M., Zhang, S.Y., Grimm, D.A., 2004. Pharmaceuticals and personal care products (PPCPs) and endocrine disrupting chemicals (EDCs) in stormwater canals and Bayou St. John in New Orleans, Louisiana, USA. Sci. Total Environ. 333, 137–148.
Brillas, E., 2020. A review on the photoelectro-Fenton process as efficient electrochemical advanced oxidation for wastewater remediation. Treatment with UV light, sunlight, and coupling with conventional and other photo-assisted advanced technologies. Chemosphere 250, 126198.
Brillas, E., Sires, I., Oturan, M.A., 2009. Electro-Fenton process and related electrochemical technologies based on Fenton's reaction chemistry. Chem. Rev. 109, 6570–6631.
Bubnov, A.G., Burova, E.Y., Grinevich, V.I., Rybkin, V.V., Kim, J.K., Choi, H.S., 2006. Plasma-catalytic decomposition of phenols in atmospheric pressure dielectric barrier discharge. Plasma Chem. Plasma Process. 26, 19–30.
Bueno, M.J.M., Gomez, M.J., Herrera, S., Hernando, M.D., Aguera, A., Fernandez-Alba, A.R., 2012. Occurrence and persistence of organic emerging contaminants and priority pollutants in five sewage treatment plants of Spain: two years pilot survey monitoring. Environ. Pollut. 164, 267–273.
Buerge, I.J., Buser, H.R., Kahle, M., Muller, M.D., Poiger, T., 2009. Ubiquitous occurrence of the artificial sweetener acesulfame in the aquatic environment: ani chemical marker of domestic wastewater in groundwater. Environ. Sci. Technol. 43, 4381–4385.

Buser, H.R., Poiger, T., Muller, M.D., 1998. Occurrence and fate of the pharmaceutical drug diclofenac in surface waters: rapid photodegradation in a lake. Environ. Sci. Technol. 32, 3449–3456.
Buser, H.R., Poiger, T., Muller, M.D., 1999. Occurrence and environmental behavior of the chiral pharmaceutical drug ibuprofen in surface waters and in wastewater. Environ. Sci. Technol. 33, 2529–2535.
Capodaglio, A.G., 2019. Contaminants of emerging concern removal by high-energy oxidation-reduction processes: state of the art. Appl. Sci. 9, 4562.
Carballa, M., Fink, G., Omil, F., Lema, J.M., Ternes, T., 2008. Determination of the solid-water distribution coefficient (K-d) for pharmaceuticals, estrogens and musk fragrances in digested sludge. Water Res. 42, 287–295.
Ceriani, E., Marotta, E., Shapoval, V., Favaro, G., Paradisi, C., 2018. Complete mineralization of organic pollutants in water by treatment with air non-thermal plasma. Chem. Eng. J. 337, 567–575.
Chen, F., Ying, G.G., Ma, Y.B., Chen, Z.F., Lai, H.J., Peng, F.J., 2014. Field dissipation and risk assessment of typical personal care products TCC, TCS, AHTN and HHCB in biosolid-amended soils. Sci. Total Environ. 470, 1078–1086.
Chen, G.H., 2004. Electrochemical technologies in wastewater treatment. Separ. Purif. Technol. 38, 11–41.
Chen, H.W., Liang, C.H., Wu, Z.M., Chang, E.E., Lin, T.F., Chiang, P.C., Wang, G.S., 2013. Occurrence and assessment of treatment efficiency of nonylphenol, octylphenol and bisphenol-A in drinking water in Taiwan. Sci. Total Environ. 449, 20–28.
Chen, X.J., Richard, J., Liu, Y.L., Dopp, E., Tuerk, J., Bester, K., 2012. Ozonation products of triclosan in advanced wastewater treatment. Water Res. 46, 2247–2256.
Clara, M., Strenn, B., Kreuzinger, N., 2004. Carbamazepine as a possible anthropogenic marker in the aquatic environment: investigations on the behaviour of Carbamazepine in wastewater treatment and during groundwater infiltration. Water Res. 38, 947–954.
Conn, K.E., Barber, L.B., Brown, G.K., Siegrist, R.L., 2006. Occurrence and fate of organic contaminants during onsite wastewater treatment. Environ. Sci. Technol. 40, 7358–7366.
Cui, T., Shen, C.Y., Xu, A.L., Han, W.Q., Li, J.S., Sun, X.Y., Shen, J.Y., Wang, L.J., 2019. Use of a novel coupled-oxidation tubular reactor (COTR)/NTP-DBD catalytic plasma in a synergistic electro-catalysis system for odorous mercaptans degradation. Chemosphere 216, 533–544.
Deblonde, T., Cossu-Leguille, C., Hartemann, P., 2011. Emerging pollutants in wastewater: a review of the literature. Int. J. Hyg Environ. Health 214, 442–448.
Decoret, C., Royer, J., Legube, B., Dore, M., 1984. Experimental and theoretical-studies of the mechanism of the initial attack of ozone on some aromatics in aqueous-medium. Environ. Technol. Lett. 5, 207–218.
Ding, S.L., Wang, X.K., Jiang, W.Q., Meng, X., Zhao, R.S., Wang, C., Wang, X., 2013. Photodegradation of the antimicrobial triclocarban in aqueous systems under ultraviolet radiation. Environ. Sci. Pollut. Res. 20, 3195–3201.
Dobrin, D., Bradu, C., Magureanu, M., Mandache, N.B., Parvulescu, V.I., 2013. Degradation of diclofenac in water using a pulsed corona discharge. Chem. Eng. J. 234, 389–396.
Dojcinovic, B.P., Roglic, G.M., Obradovic, B.M., Kuraica, M.M., Kostic, M.M., Nesic, J., Manojlovic, D.D., 2011. Decolorization of reactive textile dyes using water falling film dielectric barrier discharge. J. Hazard Mater. 192, 763–771.
Domenech, X., Ribera, M., Peral, J., 2011. Assessment of pharmaceuticals fate in a model environment. Water Air Soil Pollut. 218, 413–422.
Duan, L.J., Jiang, N., Lu, N., Shang, K.F., Li, J., Wu, Y., 2018. Synergetic effect of TiO_2 and Fe^{3+} as co-catalysts for enhanced phenol degradation in pulsed discharge system. Appl. Catal. B Environ. 221, 521–529.
Duan, X.D., He, X.X., Wang, D., Mezyk, S.P., Otto, S.C., Marfil-Vega, R., Mills, M.A., Dionysiou, D.D., 2017. Decomposition of iodinated pharmaceuticals by UV-254 nm-assisted advanced oOxidation processes. J. Hazard Mater. 323, 489–499.
E, PA U, 2021. Summary of the Safe drinking water act. https://www.epa.gov/laws-regulations/summary-safe-drinking-water-act.
Fan, J.W., Wu, H.X., Liu, R.Y., Meng, L.Y., Sun, Y.J., 2021. Review on the treatment of organic wastewater by discharge plasma combined with oxidants and catalysts. Environ. Sci. Pollut. Res. 28, 2522–2548.
Fan, Y., Ji, Y.F., Kong, D.Y., Lu, J.H., Zhou, Q.S., 2015. Kinetic and mechanistic investigations of the degradation of sulfamethazine in heat-activated persulfate oxidation process. J. Hazard Mater. 300, 39–47.
Farzadkia, M., Esrafili, A., Baghapour, M.A., Shahamat, Y.D., Okhovat, N., 2014. Degradation of metronidazole in aqueous solution by nano-ZnO/UV photocatalytic process. Desalination Water Treat. 52, 4947–4952.
Feng, J.W., Jiang, L., Zhu, D., Su, K.Z., Zhao, D.Y., Zhang, J.B., Zheng, Z., 2016. Dielectric barrier discharge plasma induced degradation of aqueous atrazine. Environ. Sci. Pollut. Res. 23, 9204–9214.
Feng, X.X., Liu, H.X., He, C., Shen, Z.X., Wang, T.B., 2018. Synergistic effects and mechanism of a non-thermal plasma catalysis system in volatile organic compound removal: a review. Catal. Sci. Technol. 8, 936–954.
Ferre, S., Ridoux, O., 2001. Searching for objects and properties with logical concept analysis. In: Delugach, H.S., Stumme, G. (Eds.), Conceptual Structures: Broadening the Base, pp. 187–201. Proceedings.
Gai, K., 2007. Plasma-induced degradation of diphenylamine in aqueous solution. J. Hazard Mater. 146, 249–254.
Gao, L.H., Sun, L., Wan, S.G., Yu, Z.B., Li, M.J., 2013. Degradation kinetics and mechanism of emerging contaminants in water by dielectric barrier discharge non-thermal plasma: the case of 17 beta-Estradiol. Chem. Eng. J. 228, 790–798.
Gao, P., Ding, Y.J., Li, H., Xagoraraki, I., 2012. Occurrence of pharmaceuticals in a municipal wastewater treatment plant: mass balance and removal processes. Chemosphere 88, 17–24.
Gerrity, D., Stanford, B.D., Trenholm, R.A., Snyder, S.A., 2010. An evaluation of a pilot-scale nonthermal plasma advanced oxidation process for trace organic compound degradation. Water Res. 44, 493–504.
Giardina, A., Tampieri, F., Marotta, E., Paradisi, C., 2018. Air non-thermal plasma treatment of Irgarol 1051 deposited on TiO_2. Chemosphere 210, 653–661.
Gong, S., Sun, Y.B., Zheng, K., Jiang, G.L., Li, L., Feng, J.W., 2020. Degradation of levofloxacin in aqueous solution by non-thermal plasma combined with Ag_3PO_4/activated carbon fibers: mechanism and degradation pathways. Separ. Purif. Technol. 250, 117264.
Gracia-Lor, E., Sancho, J.V., Serrano, R., Hernandez, F., 2012. Occurrence and removal of pharmaceuticals in wastewater treatment plants at the Spanish Mediterranean area of Valencia. Chemosphere 87, 453–462.
Gur-Reznik, S., Azerrad, S.P., Levinson, Y., Heller-Grossman, L., Dosoretz, C.G., 2011. Iodinated contrast media oxidation by nonthermal plasma: the role of iodine as a tracer. Water Res. 45, 5047–5057.
Han, J., Liu, Y.S., Singhal, N., Wang, L.Z., Gao, W., 2012. Comparative photocatalytic degradation of estrone in water by ZnO and TiO2 under artificial UVA and solar irradiation. Chem. Eng. J. 213, 150–162.
Hao, C.J., Yan, Z.Y., Liu, K.F., Qiu, J., 2020. Degradation of pharmaceutical contaminant tetracycline in aqueous solution by coaxial-type DBD plasma reactor. IEEE Trans. Plasma Sci. 48, 471–481.
Hao, H.Y., Zhang, J.L., 2009. The study of Iron (III) and nitrogen co-doped mesoporous TiO_2 photocatalysts: synthesis, characterization and activity. Microporous Mesoporous Mater. 121, 52–57.
Hartmann, J., Bartels, P., Mau, U., Witter, M., von Tumpling, W., Hofmann, J., Nietzschmann, E., 2008. Degradation of the drug diclofenac in water by sonolysis in presence of catalysts. Chemosphere 70, 453–461.
Heidler, J., Sapkota, A., Halden, R.U., 2006. Partitioning, persistence, and accumulation in digested sludge of the topical antiseptic triclocarban during wastewater treatment. Environ. Sci. Technol. 40, 3634–3639.
Heo, J., Boateng, L.K., Flora, J.R.V., Lee, H., Her, N., Park, Y.-G., Yoon, Y., 2013. Comparison of flux behavior and synthetic organic compound removal by forward osmosis and reverse osmosis membranes. J. Membr. Sci. 443, 69–82.
Hijosa-Valsero, M., Molina, R., Bayona, J.M., 2014. Assessment of a dielectric barrier discharge plasma reactor at atmospheric pressure for the removal of bisphenol A and tributyltin. Environ. Technol. 35, 1418–1426.
Hijosa-Valsero, M., Molina, R., Schikora, H., Muller, M., Bayona, J.M., 2013. Removal of priority pollutants from water by means of dielectric barrier discharge atmospheric plasma. J. Hazard Mater. 262, 664–673.
Hu, S.H., Liu, X.H., Xu, Z.M., Wang, J.Q., Li, Y.X., Shen, J., Lan, Y., Cheng, C., 2019. Degradation and mineralization of ciprofloxacin by gas-liquid discharge non-thermal plasma. Plasma Sci. Technol. 21, 015501.
Huerta-Fontela, M., Galceran, M.T., Ventura, F., 2011. Occurrence and removal of pharmaceuticals and hormones through drinking water treatment. Water Res. 45, 1432–1442.
Hyland, K.C., Dickenson, E.R.V., Drewes, J.E., Higgins, C.P., 2012. Sorption of ionized and neutral emerging trace organic compounds onto activated sludge from different wastewater treatment configurations. Water Res. 46, 1958–1968.
Ike, M., Chen, M.Y., Jin, C.S., Fujita, M., 2002. Acute toxicity, mutagenicity, and estrogenicity of biodegradation products of bisphenol-A. Environ. Toxicol. 17, 457–461.
Jankunaite, D., Tichonovas, M., Buivydiene, D., Radziuniene, I., Racys, V., Krugly, E., 2017. Removal of diclofenac, ketoprofen, and carbamazepine from simulated drinking water by advanced oxidation in a model reactor. Water Air Soil Pollut. 228, 1–15.
Jantawasu, P., Sreethawong, T., Chavadej, S., 2009. Photocatalytic activity of nanocrystalline mesoporous-assembled TiO_2 photocatalyst for degradation of methyl orange monoazo dye in aqueous wastewater. Chem. Eng. J. 155, 223–233.
Jarusutthirak, C., Amy, G., Croue, J.P., 2002. Fouling characteristics of wastewater effluent organic matter (EfOM) isolates on NF and UF membranes. Desalination 145, 247–255.
Ji, Y.F., Dong, C.X., Kong, D.Y., Lu, J.H., Zhou, Q.S., 2015. Heat-activated persulfate oxidation of atrazine: implications for remediation of groundwater contaminated by herbicides. Chem. Eng. J. 263, 45–54.
Jiang, B., Zheng, J.T., Liu, Q., Wu, M.B., 2012. Degradation of azo dye using non-thermal plasma advanced oxidation process in a circulatory airtight reactor system. Chem. Eng. J. 204, 32–39.
Jiang, B., Zheng, J.T., Qiu, S., Wu, M.B., Zhang, Q.H., Yan, Z.F., Xue, Q.Z., 2014. Review on electrical discharge plasma technology for wastewater remediation. Chem. Eng. J. 236, 348–368.
Jianjin, Hu, J., Xu, L., Wen, Y.B., Zhang, C., Meng, Y.D., Zhang, C.X., 2015. A novel TiO_2 combined pulsed diaphragm discharge system for phenol degradation. Plasma Sci. Technol. 17, 303–308.
Joseph, L., Flora, J.R.V., Park, Y.G., Badawy, M., Saleh, H., Yoon, Y., 2012. Removal of natural organic matter from potential drinking water sourcesby combined coagulation and adsorption using carbon nanomaterials. Separ. Purif. Technol. 95, 64–72.
Joseph, L., Heo, J., Park, Y.-G., Flora, J.R.V., Yoon, Y., 2011a. Adsorption of bisphenol A and 17 alpha-ethinyl estradiol on single walled carbon nanotubes from seawater and brackish water. Desalination 281, 68–74.
Joseph, L., Jun, B.M., Jang, M., Park, C.M., Munoz-Senmache, J., Hernandez-Maldonado, A.J., Heyden, A., Yoon, Y., 2019. Removal of contaminants of emerging concern by metal organic frameworks-based nanoadsorbents. Chem. Eng. J. 369, 928–946.

Joseph, L., Zaib, Q., Khan, I.A., Berge, N.D., Park, Y.-G., Saleh, N.B., Yoon, Y., 2011b. Removal of bisphenol A and 17 alpha-ethinyl estradiol from landfill leachate using single-walled carbon nanotubes. Water Res. 45, 4056–4068.
Jun, B.M., Kim, S., Heo, J., Her, N., Jang, M., Park, C.M., Yoon, Y., 2019a. Enhanced sonocatalytic degradation of carbamazepine and salicylic acid using a metal-organic framework. Ultrason. Sonochem. 56, 174–182.
Jun, B.M., Kim, S., Heo, J., Park, C.M., Her, N., Jang, M., Huang, Y., Han, J., Yoon, Y., 2019b. Review of MXenes as new nanomaterials for energy storage/delivery and selected environmental applications. Nano Res. 12, 471–487.
Jun, B.M., Park, C.M., Heo, J., Yoon, Y., 2020a. Adsorption of Ba^{2+} and Sr^{2+} from model fracking wastewater by $Ti_3C_2T_x$ MXene. J. Environ. Manag. 256, 109940.
Jun, B.M., Park, C.M., Heo, J., Yoon, Y., 2020b. Adsorption of selected dyes on $Ti_3C_2T_x$ MXene and Al-based metal-organic framework. Ceram. Int. 46, 2960–2968.
Jung, C., Oh, J., Yoon, Y., 2015. Removal of acetaminophen and naproxen by combined coagulation and adsorption using biochar: influence of combined sewer overflow components. Environ. Sci. Pollut. Res. 22, 10058–10069.
Jung, C., Park, J., Lim, K.H., Park, S., Heo, J., Her, N., Oh, J., Yun, S., Yoon, Y., 2013. Adsorption of selected endocrine disrupting compounds and pharmaceuticals on activated biochars. J. Hazard Mater. 263, 702–710.
Kasprzyk-Hordern, B., Dinsdale, R.M., Guwy, A.J., 2009. The removal of pharmaceuticals, personal care products, endocrine disruptors and illicit drugs during wastewater treatment and its impact on the quality of receiving waters. Water Res. 43, 363–380.
Kim, H.H., Teramoto, Y., Negishi, N., Ogata, A., 2015a. A multidisciplinary approach to understand the interactions of nonthermal plasma and catalyst: a review. Catal. Today 256, 13–22.
Kim, J., Coulibaly, G.N., Yoon, S., Assadi, A.A., Hanna, K., Bae, S., 2020. Red mud-activated peroxymonosulfate process for the removal of fluoroquinolones in hospital wastewater. Water Res. 184, 116171.
Kim, J.W., Yoon, S.M., Lee, S.J., Narumiya, M., Nakada, N., Han, I.S., Tanaka, H., 2012. Occurrence and fate of PPCPs wastewater treatment plants in Korea. In: 2nd International Conference on Environment and Industrial Innovation. IPCEBEE, Singapore, pp. 57–61.
Kim, K.S., Kam, S.K., Mok, Y.S., 2015b. Elucidation of the degradation pathways of sulfonamide antibiotics in a dielectric barrier discharge plasma system. Chem. Eng. J. 271, 31–42.
Kim, K.S., Yang, C.S., Mok, Y.S., 2013. Degradation of veterinary antibiotics by dielectric barrier discharge plasma. Chem. Eng. J. 219, 19–27.
Kim, S., Eichhorn, P., Jensen, J.N., Weber, A.S., Aga, D.S., 2005. Removal of antibiotics in wastewater: effect of hydraulic and solid retention times on the fate of tetracycline in the activated sludge process. Environ. Sci. Technol. 39, 5816–5823.
Kogelschatz, U., 2003. Dielectric-barrier discharges: their history, discharge physics, and industrial applications. Plasma Chem. Plasma Process. 23, 1–46.
Konstantinou, I.K., Albanis, T.A., 2004. TiO2-assisted photocatalytic degradation of azo dyes in aqueous solution: kinetic and mechanistic investigations - a review. Appl. Catal. B Environ. 49, 1–14.
Korichi, N., Aubry, O., Rabat, H., Cagnon, B., Hong, D.P., 2020. Paracetamol degradation by catalyst enhanced non-thermal plasma process for a drastic increase in the mineralization rate. Catalysts 10, 959.
Kornev, J., Yavorovsky, N., Preis, S., Khaskelberg, M., Isaev, U., Chen, B.N., 2006. Generation of active oxidant species by pulsed dielectric barrier discharge in water-air mixtures. Ozone: Sci. Eng. 28, 207–215.
Kovalakova, P., Cizmas, L., McDonald, T.J., Marsalek, B., Feng, M.B., Sharma, V.K., 2020. Occurrence and toxicity of antibiotics in the aquatic environment: a review. Chemosphere 251, 126351.
Krause, H., Schweiger, B., Prinz, E., Kim, J., Steinfeld, U., 2011. Degradation of persistent pharmaceuticals in aqueous solutions by a positive dielectric barrier discharge treatment. J. Electrost. 69, 333–338.
Krause, H., Schweiger, B., Schuhmacher, J., Scholl, S., Steinfeld, U., 2009. Degradation of the endocrine disrupting chemicals (EDCs) carbamazepine, clofibric acid, and iopromide by corona discharge over water. Chemosphere 75, 163–168.
Krishna, S., Ceriani, E., Marotta, E., Giardina, A., Spatenka, P., Paradisi, C., 2016. Products and mechanism of verapamil removal in water by air non-thermal plasma treatment. Chem. Eng. J. 292, 35–41.
Lei, H.X., Snyder, S.A., 2007. 3D QSPR models for the removal of trace organic contaminants by ozone and free chlorine. Water Res. 41, 4051–4060.
Leitner, N.K.V., Syoen, G., Romat, H., Urashima, K., Chang, J.S., 2005. Generation of active entities by the pulsed arc electrohydraulic discharge system and application to removal of atrazine. Water Res. 39, 4705–4714.
Liang, C.J., Wang, Z.S., Mohanty, N., 2006. Influences of carbonate and chloride ions on persulfate oxidation of trichloroethylene at 20 degrees C. Sci. Total Environ. 370, 271–277.
Liu, C., Nanaboina, V., Korshin, G.V., Jiang, W.J., 2012a. Spectroscopic study of degradation products of ciprofloxacin, norfloxacin and lomefloxacin formed in ozonated wastewater. Water Res. 46, 5235–5246.
Liu, S., Hu, C., Wei, Y., Duan, M., Chen, X., Hu, Y., 2018. Transformation of H-aggregates and J-dimers of water-soluble tetrakis (4-carboxyphenyl) porphyrin in polyion complex micelles. Polymers 10, 494.
Liu, Y.J., Sun, L., Wu, J., Fang, T., Cai, R., Wei, A., 2015. Preparation and photocatalytic activity of ZnO/Fe_2O_3 nanotube composites. Mater. Sci. Eng. B 194, 9–13.
Liu, Y.N., Mei, S.F., Iya-Sou, D., Cavadias, S., Ognier, S., 2012b. Carbamazepine removal from water by dielectric barrier discharge: comparison of ex situ and in situ discharge on water. Chem. Eng. Process 56, 10–18.
Liu, Y.N., Wang, C.H., Shen, X., Zhang, A., Yan, S.W., Li, X., Miruka, A.C., Wu, S.M., Guo, Y., Ognier, S., 2019. Degradation of glucocorticoids in aqueous solution by dielectric barrier discharge: kinetics, mechanisms, and degradation pathways. Chem. Eng. J. 374, 412–428.
Liu, Y.N., Zhu, S.F., Tian, H., Zhou, M., Miao, J., 2013. Effect of inorganic ions on the oxidation of methyl violet with gliding arc plasma discharge. Plasma Chem. Plasma Process. 33, 737–749.
Liu, Z.-h., Kanjo, Y., Mizutani, S., 2009. Removal mechanisms for endocrine disrupting compounds (EDCs) in wastewater treatment - physical means, biodegradation, and chemical advanced oxidation: a review. Sci. Total Environ. 407, 731–748.
Locke, B.R., Thagard, S.M., 2012. Analysis and review of chemical reactions and transport processes in pulsed electrical discharge plasma formed directly in liquid water. Plasma Chem. Plasma Process. 32, 875–917.
Lou, J., Wei, Y., Zhang, M.H., Meng, Q., An, J.T., Jia, M.K., 2021. Removal of tetracycline hydrochloride in aqueous by coupling dielectric barrier discharge plasma with biochar. Separ. Purif. Technol. 266, 118515.
Lukes, P., Clupek, M., Babicky, V., Janda, V., Sunka, P., 2005. Generation of ozone by pulsed corona discharge over water surface in hybrid gas-liquid electrical discharge reactor. J. Phys. D Appl. Phys. 38, 409–416.
Luo, Y., Guo, W., Ngo, H.H., Long Duc, N., Hai, F.I., Zhang, J., Liang, S., Wang, X.C., 2014. A review on the occurrence of micropollutants in the aquatic environment and their fate and removal during wastewater treatment. Sci. Total Environ. 473, 619–641.
Magureanu, M., Mandache, N.B., Bradu, C., Parvulescu, V.I., 2018. High efficiency plasma treatment of water contaminated with organic compounds. Study of the degradation of ibuprofen. Plasma Process. Polym. 15, 201.
Magureanu, M., Piroi, D., Mandache, N.B., David, V., Medvedovici, A., Bradu, C., Parvulescu, V.I., 2011. Degradation of antibiotics in water by non-thermal plasma treatment. Water Res. 45, 3407–3416.
Magureanu, M., Piroi, D., Mandache, N.B., David, V., Medvedovici, A., Parvulescu, V.I., 2010. Degradation of pharmaceutical compound pentoxifylline in water by non-thermal plasma treatment. Water Res. 44, 3445–3453.
Malik, M.A., 2010. Water purification by plasmas: which reactors are most energy efficient? Plasma Chem. Plasma Process. 30, 21–31.
Markovic, M., Jovic, M., Stankovic, D., Kovacevic, V., Roglic, G., Gojgic-Cvijovic, G., Manojlovic, D., 2015. Application of non-thermal plasma reactor and Fenton reaction for degradation of ibuprofen. Sci. Total Environ. 505, 1148–1155.
Maruthi, Y.A., Lakshmana Das, N., Hossain, K., Sarma, K.S.S., Rawat, K.S., Sabharwal, S., 2011. Disinfection and reduction of organic load of sewage water by electron beam radiation. Appl. Water Sci. 1, 49–56.
Matsuno, T., Matsukawa, T., Sakuma, Y., Kunieda, T., 1989. A new nitration product, 3-nitro-4-acetamidophenol, obtained from acetaminophen with nitrrous-acid Chem. Pharm. Bull. 37, 1422–1423.
Mawhinney, D.B., Young, R.B., Vanderford, B.J., Borch, T., Snyder, S.A., 2011. Artificial sweetener sucralose in U.S. drinking water systems. Environ. Sci. Technol. 45, 8716–8722.
Mededovic Thagard, S., Stratton, G.R., Dai, F., Bellona, C.L., Holsen, T.M., Bohl, D.G., Paek, E., Dickenson, E.R.V., 2016. Plasma-based water treatment: development of a general mechanistic model to estimate the treatability of different types of contaminants. J. Phys. D Appl. Phys. 50, 014003.
Mehrjouei, M., Muller, S., Moller, D., 2014. Catalytic and photocatalytic ozonation of tert-butyl alcohol in water by means of falling film reactor: kinetic and cost-effectiveness study. Chem. Eng. J. 248, 184–190.
Meyer, J., Bester, K., 2004. Organophosphate flame retardants and plasticisers in wastewater treatment plants. J. Environ. Monit. 6, 599–605.
Mohapatra, S., Huang, C.H., Mukherji, S., Padhye, L.P., 2016. Occurrence and fate of pharmaceuticals in WWTPs in India and comparison with a similar study in the United States. Chemosphere 159, 526–535.
Moreira, N.F.F., Orge, C.A., Ribeiro, A.R., Faria, J.L., Nunes, O.C., Pereira, M.F.R., Silva, A.M.T., 2015. Fast mineralization and detoxification of amoxicillin and diclofenac by photocatalytic ozonation and application to an urban wastewater. Water Res. 87, 87–96.
Nam, S.W., Jung, C., Li, H., Yu, M., Flora, J.R.V., Boateng, L.K., Her, N., Zoh, K.D., Yoon, Y., 2015. Adsorption characteristics of diclofenac and sulfamethoxazole to graphene oxide in aqueous solution. Chemosphere 136, 20–26.
Ngundi, M.M., Sadik, O.A., Yamaguchi, T., Suye, S., 2003. First comparative reaction mechanisms of beta-estradiol and selected environmental hormones in a redox environment. Electrochem. Commun. 5, 61–67.
Ognier, S., Iya-sou, D., Fourmond, C., Cavadias, S., 2009. Analysis of mechanisms at the plasma-liquid interface in a gas-liquid discharge reactor used for treatment of polluted water. Plasma Chem. Plasma Process. 29, 261–273.
Ohko, Y., Ando, I., Niwa, C., Tatsuma, T., Yamamura, T., Nakashima, T., Kubota, Y., Fujishima, A., 2001. Degradation of bisphenol A in water by TiO_2 photocatalyst. Environ. Sci. Technol. 35, 2365–2368.
Ono, R., Oda, T., 2002. Dynamics and density estimation of hydroxyl radicals in a pulsed corona discharge. J. Phys. D Appl. Phys. 35, 2133–2138.
Ormad, M.P., Miguel, N., Claver, A., Matesanz, J.M., Ovelleiro, J.L., 2008. Pesticides removal in the process of drinking water production. Chemosphere 71, 97–106.
Pan, X.Y., Qiao, X.C., 2019. Influences of nitrite on paracetamol degradation in dielectric barrier discharge reactor. Ecotoxicol. Environ. Saf. 180, 610–615.
Park, C., Fang, Y., Murthy, S.N., Novak, J.T., 2010. Effects of floc aluminum on activated sludge characteristics and removal of 17-alpha-ethinylestradiol in wastewater systems. Water Res. 44, 1335–1340.
Pera-Titus, M., Garcia-Molina, V., Banos, M.A., Gimenez, J., Esplugas, S., 2004. Degradation of chlorophenols by means of advanced oxidation processes: a general review. Appl. Catal. B Environ. 47, 219–256.
Perez-Estrada, L.A., Malato, S., Gernjak, W., Aguera, A., Thurman, E.M., Ferrer, I., Fernandez-Alba, A.R., 2005. Photo-fenton degradation of diclofenac: identification

of main intermediates and degradation pathway. Environ. Sci. Technol. 39, 8300–8306.
Phillips, P.J., Chalmers, A.T., Gray, J.L., Kolpin, D.W., Foreman, W.T., Wall, G.R., 2012. Combined sewer overflows: an environmental source of hormones and wastewater micropollutants. Environ. Sci. Technol. 46, 5336–5343.
Piera, E., Calpe, J.C., Brillas, E., Domenech, X., Peral, J., 2000. 2,4-Dichlorophenoxyacetic acid degradation by catalyzed ozonation: TiO_2/UVA/O^3 and Fe(II)/UVA/O^3 systems. Appl. Catal. B Environ. 27, 169–177.
Piskarev, I.M., Astaf'eva, K.A., Ivanova, I.P., 2018. Sources of gas-discharge plasma: effect of the absorbed dose and active particle composition on physicochemical transformations in biological substrates. Sovrem. Technol. v Med. 10, 90–99.
Puertas, E.C., Peyot, M.L., Pineda, M., Volk, K., Coulombe, S., Yargeau, V., 2021. Degradation of diatrizoate in a pin-to-liquid plasma reactor, its transformation products and their residual toxicity. Sci. Total Environ. 782, 146895.
Rahimi, S., Ayati, B., Rezaee, A., 2016. Kinetic modeling and determination role of sono/photo nanocatalyst-generated radical species on degradation of hydroquinone in aqueous solution. Environ. Sci. Pollut. Res. 23, 12185–12198.
Rao, Y.F., Yang, H.S., Xue, D., Guo, Y., Qi, F., Ma, J., 2016. Sonolytic and sonophotolytic degradation of carbamazepine: kinetic and mechanisms. Ultrason. Sonochem. 32, 371–379.
Reddy, P.M.K., Mahammadunnisa, S., Subrahmanyam, C., 2014. Catalytic non-thermal plasma reactor for mineralization of endosulfan in aqueous medium: a green approach for the treatment of pesticide contaminated water. Chem. Eng. J. 238, 157–163.
Reddy, P.M.K., Subrahmanyam, C., 2015. Catalytic plasma reactor for degradation and mineralization of pharmaceuticals and personal care products. J. Adv. Oxid. 18, 161–166.
Reemtsma, T., Miehe, U., Duennbier, U., Jekel, M., 2010. Polar pollutants in municipal wastewater and the water cycle: occurrence and removal of benzotriazoles. Water Res. 44, 596–604.
Rong, S.P., Sun, Y.B., Zhao, Z.H., 2014. Degradation of sulfadiazine antibiotics by water falling film dielectric barrier discharge. Chin. Chem. Lett. 25, 187–192.
Russo, M., Iervolino, G., Vaiano, V., Palma, V., 2020. Non-thermal plasma coupled with catalyst for the degradation of water pollutants: a review. Catalysts 10, 1438.
Ryu, J., Oh, J., Snyder, S.A., Yoon, Y., 2014. Determination of micropollutants in combined sewer overflows and their removal in a wastewater treatment plant (Seoul, South Korea). Environ. Monit. Assess. 186, 3239–3251.
Ryu, J., Yoon, Y., Oh, J., 2011. Occurrence of endocrine disrupting compounds and pharmaceuticals in 11 WWTPs in Seoul, Korea. KSCE J. Civil. Eng. 15, 57–64.
Sarangapani, C., Danaher, M., Tiwari, B., Lu, P., Bourke, P., Cullen, P.J., 2017a. Efficacy and mechanistic insights into endocrine disruptor degradation using atmospheric air plasma. Chem. Eng. J. 326, 700–714.
Sarangapani, C., Dixit, Y., Milosavljevic, V., Bourke, P., Sullivan, C., Cullen, P.J., 2017b. Optimization of atmospheric air plasma for degradation of organic dyes in wastewater. Water Sci. Technol. 75, 207–219.
Sarangapani, C., Ziuzina, D., Behan, P., Boehm, D., Gilmore, B.F., Cullen, P.J., Bourke, P., 2019. Degradation kinetics of cold plasma-treated antibiotics and their antimicrobial activity. Sci. Rep. 9, 3955.
Serna-Galvis, E.A., Silva-Agredo, J., Giraldo-Aguirre, A.L., Florez-Acosta, O.A., Torres-Palma, R.A., 2016. High frequency ultrasound as a selective advanced oxidation process to remove penicillinic antibiotics and eliminate its antimicrobial activity from water. Ultrason. Sonochem. 31, 276–283.
Sichel, C., Garcia, C., Andre, K., 2011. Feasibility studies: UV/chlorine advanced oxidation treatment for the removal of emerging contaminants. Water Res. 45, 6371–6380.
Sim, W.J., Lee, J.W., Lee, E.S., Shin, S.K., Hwang, S.R., Oh, J.E., 2011. Occurrence and distribution of pharmaceuticals in wastewater from households, livestock farms, hospitals and pharmaceutical manufactures. Chemosphere 82, 179–186.
Singh, R.K., Babu, V., Philip, L., Ramanujam, S., 2016. Applicability of pulsed power technique for the degradation of methylene blue. J. Water Proc. Eng. 11, 118–129.
Singh, R.K., Philip, L., Ramanujam, S., 2017a. Rapid degradation, mineralization and detoxification of pharmaceutically active compounds in aqueous solution during pulsed corona discharge treatment. Water Res. 121, 20–36.
Singh, R.K., Philip, L., Ramanujam, S., 2017b. Removal of 2,4-dichlorophenoxyacetic acid in aqueous solution by pulsed corona discharge treatment: effect of different water constituents, degradation pathway and toxicity assay. Chemosphere 184, 207–214.
Singh, R.K., Philip, L., Ramanujam, S., 2019. Continuous flow pulse corona discharge reactor for the tertiary treatment of drinking water: insights on disinfection and emerging contaminants removal. Chem. Eng. J. 355, 269–278.
Snyder, E.H., O'Connor, G.A., 2013. Risk assessment of land-applied biosolids-borne triclocarban (TCC). Sci. Total Environ. 442, 437–444.
Snyder, E.H., O'Connor, G.A., McAvoy, D.C., 2011. Toxicity and bioaccumulation of biosolids-borne triclocarban (TCC) in terrestrial organisms. Chemosphere 82, 460–467.
Snyder, S., Leising, J., Westerhoff, P., Yoon, Y., Mash, H., Vanderford, B., 2004. Biological and physical attenuation of endocrine disruptors and pharmaceuticals: implications for water reuse. Ground Water Monit. Remediat 24, 108–118.
Snyder, S.A., Adham, S., Redding, A.M., Cannon, F.S., DeCarolis, J., Oppenheimer, J., Wert, E.C., Yoon, Y., 2007. Role of membranes and activated carbon in the removal of endocrine disruptors and pharmaceuticals. Desalination 202, 156–181.
Snyder, S.A., Westerhoff, P., Yoon, Y., Sedlak, D.L., 2003. Pharmaceuticals, personal care products, and endocrine disruptors in water: implications for the water industry. Environ. Eng. Sci. 20, 449–469.
Stackelberg, P.E., Gibs, J., Furlong, E.T., Meyer, M.T., Zaugg, S.D., Lippincott, R.L., 2007. Efficiency of conventional drinking-water-treatment processes in removal of pharmaceuticals and other organic compounds. Sci. Total Environ. 377, 255–272.
Staehelin, J., Buhler, R.E., Hoigne, J., 1984. Ozone decomposition in water studied by pulse-radiolysis. OH and HO4 as chain intermediates. J. Phys. Chem. 88, 5999–6004.
Stratton, G.R., Bellona, C.L., Dai, F., Holsen, T.M., Thagard, S.M., 2015. Plasma-based water treatment: conception and application of a new general principle for reactor design. Chem. Eng. J. 273, 543–550.
Stumm-Zollinger, E., Fair, G.M., 1965. Biodegradation of steroid hormones. J. Water Pollut. Cont. 37, 1506–1510.
Sudakin, D.L., Trevathan, W.R., 2003. DEET: a review and update of safety and risk in the general population. J. Toxicol. Clin. Toxicol. 41, 831–839.
Sui, Q., Huang, J., Deng, S., Yu, G., Fan, Q., 2010. Occurrence and removal of pharmaceuticals, caffeine and DEET in wastewater treatment plants of Beijing, China. Water Res. 44, 417–426.
Sun, B., Sato, M., Clements, J.S., 1997. Optical study of active species produced by a pulsed streamer corona discharge in water. J. Electrost. 39, 189–202.
Sun, B., Sato, M., Clements, J.S., 1999. Use of a pulsed high-voltage discharge for removal of organic compounds in aqueous solution. J. Phys. D Appl. Phys. 32, 1908–1915.
Takahashi, K., Satoh, K., Itoh, H., Kawaguchi, H., Timoshkin, I., Given, M., MacGregor, S., 2016. Production characteristics of reactive oxygen/nitrogen species in water using atmospheric pressure discharge plasmas. Jpn. J. Appl. Phys. 55, 07LF01.
Tan, C.Q., Gao, N.Y., Deng, Y., An, N., Deng, J., 2012. Heat-activated persulfate oxidation of diuron in water. Chem. Eng. J. 203, 294–300.
Tang, S.F., Li, N., Qi, J.B., Yuan, D.L., Li, J., 2018a. Degradation of phenol using a combination of granular activated carbon adsorption and bipolar pulse dielectric barrier discharge plasma regeneration. Plasma Sci. Technol. 20, 054013.
Tang, S.F., Lu, N., Li, J., Wu, Y., 2012. Removal of bisphenol A in water using an integrated granular activated carbon preconcentration and dielectric barrier discharge degradation treatment. Thin Solid Films 521, 257–260.
Tang, S.F., Yuan, D.L., Rao, Y.D., Li, M.H., Shi, G.M., Gu, J.M., Zhang, T.H., 2019. Percarbonate promoted antibiotic decomposition in dielectric barrier discharge plasma. J. Hazard Mater. 366, 669–676.
Tang, S.F., Yuan, D.L., Rao, Y.D., Li, N., Qi, J.B., Cheng, T.Z., Sun, Z.T., Gu, J.M., Huang, H.M., 2018b. Persulfate activation in gas phase surface discharge plasma for synergetic removal of antibiotic in water. Chem. Eng. J. 337, 446–454.
Tay, K.S., Abd Rahman, N., Bin Abas, M.R., 2012. Degradation of bisphenol A by ozonation: rate constants, influence of inorganic anions, and by-products. Maejo Int. J. Sci. Technol. 6, 77–94.
Ternes, T.A., Meisenheimer, M., McDowell, D., Sacher, F., Brauch, H.J., Gulde, B.H., Preuss, G., Wilme, U., Seibert, N.Z., 2002. Removal of pharmaceuticals during drinking water treatment. Environ. Sci. Technol. 36, 3855–3863.
Tian, C., Liu, R.P., Liu, H.J., Qu, J.H., 2013. Disinfection by-products formation and precursors transformation during chlorination and chloramination of highly-polluted source water: significance of ammonia. Water Res. 47, 5901–5910.
Torres, C.I., Ramakrishna, S., Chiu, C.A., Nelson, K.G., Westerhoff, P., Krajmalnik-Brown, R., 2011. Fate of sucralose during wastewater treatment. Environ. Eng. Sci. 28, 325–331.
U.S. Department of the Interior, B.o.R., 2009. Review on the treatment of organic wastewater by discharge plasma combined with oxidants and catalysts (Secondary/Emerging Constituents Report).
USEPA, 2000. Environmental Protection Agency - Endocrine Disruptor Screening Program. USEPA, Washington, DC. Report to Congress.
USEPA, 2016. Contaminant Candidate List (CCL) and Regulatory Determination - CCL4. https://www.epa.gov/ccl/contaminant-candidate-list-4-ccl-4-0.
Vanraes, P., Willems, G., Daels, N., Van Hulle, S.W.H., De Clerck, K., Surmont, P., Lynen, F., Vandamme, J., Van Durme, J., Nikiforov, A., Leys, C., 2015a. Decomposition of atrazine traces in water by combination of non-thermal electrical discharge and adsorption on nanofiber membrane. Water Res. 72, 361–371.
Vanraes, P., Willems, G., Nikiforov, A., Surmont, P., Lynen, F., Vandamme, J., Van Durme, J., Verheust, Y.P., Van Hulle, S.W.H., Dumoulin, A., Leys, C., 2015b. Removal of atrazine in water by combination of activated carbon and dielectric barrier discharge. J. Hazard Mater. 299, 647–655.
Vieno, N., Sillanpaa, M., 2014. Fate of diclofenac in municipal wastewater treatment plant - a review. Environ. Int. 69, 28–39.
Vonsonntag, C., Schuchmann, H.P., 1991. The elucidation of peroxyl radical reactions in aqueous-solution with the help of radition-chemical methods. Angew. Chem. Int. Ed. Engl. 30, 1229–1253.
Walsh, J.L., Bruggeman, P., 2011. Filamentation of diffuse He-H_2O atmospheric pressure glow discharges in a metal pin-water electrode geometry. IEEE Trans. Plasma Sci. 39, 2634–2635.
Wang, B.W., Wang, C., Yao, S.M., Peng, Y.P., Xu, Y., 2019. Plasma-catalytic degradation of tetracycline hydrochloride over Mn/gamma-Al2O3 catalysts in a dielectric barrier discharge reactor. Plasma Sci. Technol. 21, 065503.
Wang, C., Qu, G.Z., Wang, T.C., Deng, F., Liang, D.L., 2018. Removal of tetracycline antibiotics from wastewater by pulsed corona discharge plasma coupled with natural soil particles. Chem. Eng. J. 346, 159–170.
Wang, J., Sun, Y.B., Feng, J.W., Xin, L., Ma, J.Z., 2016a. Degradation of triclocarban in water by dielectric barrier discharge plasma combined with TiO_2/activated carbon fibers: effect of operating parameters and byproducts identification. Chem. Eng. J. 300, 36–46.
Wang, J., Sun, Y.B., Jiang, H., Feng, J.W., 2017a. Removal of caffeine from water by combining dielectric barrier discharge (DBD) plasma with goethite. J. Saudi Chem. Soc. 21, 545–557.

Wang, J.L., Wang, S.Z., 2018. Activation of persulfate (PS) and peroxymonosulfate (PMS) and application for the degradation of emerging contaminants. Chem. Eng. J. 334, 1502–1517.
Wang, J.Q., Zheng, B.G., Zhang, J.B., Zheng, Z., 2013. Degradation of the emerging contaminant naproxen in aqueous solutions by dielectric barrier discharge. Chem. Asian J. 25, 3595–3600.
Wang, L., Jiang, X.Z., Liu, Y.J., 2008. Degradation of bisphenol A and formation of hydrogen peroxide induced by glow discharge plasma in aqueous solutions. J. Hazard Mater. 154, 1106–1114.
Wang, L., Sun, L., Yu, Z.B., Hou, Y.P., Peng, Z.B., Yang, F., Chen, Y., Huang, J., 2017b. Synergetic decomposition performance and mechanism of perfluorooctanoic acid in dielectric barrier discharge plasma system with Fe_3O_4@SiO_2-BiOBr magnetic photocatalyst. Mol. Catal. 441, 179–189.
Wang, L., Yi, Y.H., Zhao, Y., Zhang, R., Zhang, J.L., Guo, H.C., 2015. NH_3 decomposition for H_2 generation: effects of cheap metals and supports on plasma-catalyst synergy. ACS Catal. 5, 4167–4174.
Wang, Q.C., Zhang, A., Li, P., Heroux, P.H., Zhang, H., Yu, X., Liu, Y.A., 2021. Degradation of aqueous atrazine using persulfate activated by electrochemical plasma coupling with microbubbles: removal mechanisms and potential applications. J. Hazard Mater. 403, 124087.
Wang, T.C., Qu, G.Z., Ren, J.Y., Sun, Q.H., Liang, D.L., Hu, S.B., 2016b. Organic acids enhanced decoloration of azo dye in gas phase surface discharge plasma system. J. Hazard Mater. 302, 65–71.
Wardenier, N., Vanraes, P., Nikiforov, A., Van Hulle, S.W.H., Leys, C., 2019. Removal of micropollutants from water in a continuous-flow electrical discharge reactor. J. Hazard Mater. 362, 238–245.
Westerhoff, P., Moon, H., Minakata, D., Crittenden, J., 2009. Oxidation of organics in retentates from reverse osmosis wastewater reuse facilities. Water Res. 43, 3992–3998.
Westerhoff, P., Yoon, Y., Snyder, S., Wert, E., 2005. Fate of endocrine-disruptor, pharmaceutical, and personal care product chemicals during simulated drinking water treatment processes. Environ. Sci. Technol. 39, 6649–6663.
Weyrauch, P., Matzinger, A., Pawlowsky-Reusing, E., Plume, S., von Seggern, D., Heinzmann, B., Schroeder, K., Rouault, P., 2010. Contribution of combined sewer overflows to trace contaminant loads in urban streams. Water Res. 44, 4451–4462.
Wu, C.X., Spongberg, A.L., Witter, J.D., Fang, M., Czajkowski, K.P., Ames, A., 2010. Dissipation and leaching potential of selected pharmaceutically active compounds in soils amended with biosolids. Arch. Environ. Contam. Toxicol. 59, 343–351.
Wu, H.X., Fan, J.W., Chen, W.G., Yang, C.W., 2020. Dielectric barrier discharge-coupled Fe-based zeolite to remove ammonia nitrogen and phenol pollutants from water. Separ. Purif. Technol. 243, 116344.
Xin, L., Sun, Y.B., Feng, J.W., Wang, J., He, D., 2016. Degradation of triclosan in aqueous solution by dielectric barrier discharge plasma combined with activated carbon fibers. Chemosphere 144, 855–863.
Xu, X.H., Lu, Y., Zhang, G.X., Chen, L., Tian, D., Shen, X.Y., Yang, Y.L., Dong, F.N., 2014. Bisphenol A promotes dendritic morphogenesis of hippocampal neurons through estrogen receptor-mediated ERK1/2 signal pathway. Chemosphere 96, 129–137.
Xu, Z.M., Xue, X.J., Hu, S.H., Li, Y.X., Shen, J., Lan, Y., Zhou, R.X., Yang, F., Cheng, C., 2020. Degradation effect and mechanism of gas-liquid phase dielectric barrier discharge on norfloxacin combined with H_2O_2 or Fe^{2+}. Separ. Purif. Technol. 230, 115862.
Yang, B., Ying, G.-G., Zhao, J.-L., Liu, S., Zhou, L.-J., Chen, F., 2012. Removal of selected endocrine disrupting chemicals (EDCs) and pharmaceuticals and personal care products (PPCPs) during ferrate(VI) treatment of secondary wastewater effluents. Water Res. 46, 2194–2204.
Yoon, Y., Ryu, J., Oh, J., Choi, B.G., Snyder, S.A., 2010. Occurrence of endocrine disrupting compounds, pharmaceuticals, and personal care products in the Han River (Seoul, South Korea). Sci. Total Environ. 408, 636–643.
Yoon, Y., Westerhoff, P., Snyder, S.A., Wert, E.C., 2006. Nanofiltration and ultrafiltration of endocrine disrupting compounds, pharmaceuticals and personal care products. J. Membr. Sci. 270, 88–100.
Yoon, Y., Westerhoff, P., Snyder, S.A., Wert, E.C., Yoon, J., 2007. Removal of endocrine disrupting compounds and pharmaceuticals by nanofiltration and ultrafiltration membranes. Desalination 202, 16–23.
Yoon, Y.M., Westerhoff, P., Snyder, S.A., Esparza, M., 2003. HPLC-fluorescence detection and adsorption of bisphenol A, 17 beta-estradiol, and 17 alpha-ethynyl estradiol on powdered activated carbon. Water Res. 37, 3530–3537.
Yu, Z.Q., Sun, Y.B., Zhang, G.Y., Zhang, C.X., 2017. Degradation of DEET in aqueous solution by water falling film dielectric barrier discharge : effect of three operating modes and analysis of the mechanism and degradation pathway. Chem. Eng. J. 317, 90–102.
Zaib, Q., Khan, I.A., Saleh, N.B., Flora, J.R.V., Park, Y.-G., Yoon, Y., 2012. Removal of bisphenol A and 17 beta-estradiol by single-walled carbon nanotubes in aqueous solution: adsorption and molecular modeling. Water Air Soil Pollut. 223, 3281–3293.
Zhang, G.Y., Sun, Y.B., Zhang, C.X., Yu, Z.Q., 2017a. Decomposition of acetaminophen in water by a gas phase dielectric barrier discharge plasma combined with TiO2-rGO nanocomposite: mechanism and degradation pathway. J. Hazard Mater. 323, 719–729.
Zhang, H., Huang, Q., Li, L.M., Ke, Z.G., Wang, Q., 2016. Distinguish the role of DBD-accompanying UV-radiation in the degradation of bisphenol A. Plasma Chem. Plasma Process. 36, 585–598.
Zhang, H., Zhang, Q.F., Miao, C.G., Huang, Q., 2018a. Degradation of 2, 4-dichloro-phenol in aqueous solution by dielectric barrier discharge: effects of plasma-working gases, degradation pathways and toxicity assessment. Chemosphere 204, 351–358.
Zhang, Q.F., Zhang, H., Zhang, Q.X., Huang, Q., 2018b. Degradation of norfloxacin in aqueous solution by atmospheric-pressure non-thermal plasma: mechanism and degradation pathways. Chemosphere 210, 433–439.
Zhang, Q.R., Qu, G.Z., Wang, T.C., Li, C.G., Qiang, H., Sun, Q.H., Liang, D.L., Hu, S.B., 2017b. Humic acid removal from micro-polluted source water in the presence of inorganic salts in a gas-phase surface discharge plasma system. Separ. Purif. Technol. 187, 334–342.
Zhang, X., Wu, F., Wu, X.W., Chen, P.Y., Deng, N.S., 2008. Photodegradation of acetaminophen in TiO2 suspended solution. J. Hazard Mater. 157, 300–307.
Zhang, Y., Lu, J.N., Wang, X.P., Xin, Q., Cong, Y.Q., Wang, Q., Li, C.J., 2013. Phenol degradation by $_{TiO2}$ photocatalysts combined with different pulsed discharge systems. J. Colloid Interface Sci. 409, 104–111.
Zhang, Z.F., Ren, N.Q., Li, Y.F., Kunisue, T., Gao, D.W., Kannan, K., 2011. Determination of benzotriazole and benzophenone UV filters in sediment and sewage sludge. Environ. Sci. Technol. 45, 3909–3916.